On the impact of power corrections in the prediction of $B \to K^* \mu^+ \mu^-$ observables

Sébastien Descotes-Genon,[a] Lars Hofer,[b] Joaquim Matias[b] and Javier Virto[c]

[a]*Laboratoire de Physique Théorique, CNRS/Univ. Paris-Sud 11 (UMR 8627)*
91405 Orsay Cedex, France

[b]*Universitat Autònoma de Barcelona,*
08193 Bellaterra, Barcelona

[c]*Theoretische Physik 1, Naturwissenschaftlich-Technische Fakultät,*
Universität Siegen, 57068 Siegen, Germany

E-mail: sebastien.descotes-genon@th.u-psud.fr, lhofer@ifae.es, matias@ifae.es, virto@physik.uni-siegen.de

Abstract: The recent LHCb angular analysis of the exclusive decay $B \to K^* \mu^+ \mu^-$ has indicated significant deviations from the Standard Model expectations. Accurate predictions can be achieved at large K^*-meson recoil for an optimised set of observables designed to have no sensitivity to hadronic input in the heavy-quark limit at leading order in α_s. However, hadronic uncertainties reappear through non-perturbative $\Lambda_{\rm QCD}/m_b$ power corrections, which must be assessed precisely. In the framework of QCD factorisation we present a systematic method to include factorisable power corrections and point out that their impact on angular observables depends on the scheme chosen to define the soft form factors. Associated uncertainties are found to be under control, contrary to earlier claims in the literature. We also discuss the impact of possible non-factorisable power corrections, including an estimate of charm-loop effects. We provide results for angular observables at large recoil for two different sets of inputs for the form factors, spelling out the different sources of theoretical uncertainties. Finally, we comment on a recent proposal to explain the anomaly in $B \to K^* \mu^+ \mu^-$ observables through charm-resonance effects, and we propose strategies to test this proposal identifying observables and kinematic regions where either the charm-loop model can be disentangled from New Physics effects or the two options leave different imprints.

Contents

1 Introduction

Since many years, radiative transitions $b \to s\gamma^{(*)}$ have been considered as very powerful probes of physics beyond the Standard Model (SM). These Flavour-Changing Neutral Currents (FCNC) are only mediated by loops in the Standard Model and thus exhibit a quantum sensitivity to New Physics (NP). Recently the exclusive decay $B \to K^* \mu^+ \mu^-$ has come to prominence, as the latest LHCb angular analysis [1, 2] suggests significant deviations from the Standard Model, most notably in the observables P_5' [3] and P_2 [4, 5] in the region of large hadronic recoil. Within the model-independent effective Hamiltonian approach (summarised for instance in ref. [6]), it has been shown in ref. [7] that such deviations can be easily accommodated in the presence of short-distance NP contributions to the semileptonic operator O_9, reducing the size of the Wilson coefficient C_9 by 25% with respect to the SM prediction.

Several later studies have reached similar conclusions from $B \to K^* \mu^+ \mu^-$ data, using different observables [8] and/or statistical methods [9], with possible interpretations in terms of Z' models[1] [7, 8, 18–21]. Interestingly, a recent lattice study of $B \to K^* \mu^+ \mu^-$ and $B_s \to \phi \mu^+ \mu^-$ form factors [22, 23] confirms the same trend using different observables (branching ratios rather than angular observables) and in a different kinematic regime (low rather than large hadronic recoil). The need for NP contributions to other operators, and in particular to the chirality-flipped semileptonic operator O_9', is currently debated depending on the subset of observables and bins chosen and the input for hadronic form factors [7–9, 23, 24]. Another issue currently debated is the exact role of long-distance $c\bar{c}$ loops, for which only partial estimates exist [25], pushing in the opposite direction to LHCb data, i.e. making the anomaly more severe [7]. A comparison of BES data on $\sigma(e^+ e^- \to \text{hadrons})$ [26] and the $B^+ \to K^+ \mu^+ \mu^-$ dimuon spectrum [27] suggests that non-factorisable corrections above the $c\bar{c}$ threshold are very large [28]. Dispersive approaches have been used to exploit this information and to estimate the effects in $B \to K^* \mu^+ \mu^-$ [28], but it remains unclear how reliable these methods are in reconstructing the needed real and imaginary parts of the $c\bar{c}$ loop function (including all long-distance effects) at low recoil, as well as its extrapolation to the large-recoil region (see appendix for further discussion).

A usual problem in quark flavour physics is the precise estimation of hadronic uncertainties, necessary for a correct comparison between theory and data. Reliable constraints on short-distance Wilson coefficients depend on that premise, as well as the statistical assessment of deviations potentially related to NP. This can only be achieved if long-distance effects, encoded for example in hadronic form factors, are sufficiently under control. Although calculations with different non-perturbative methods are available, e.g., light-cone sum rules (LCSR) at large recoil and lattice QCD at low recoil, they have not yet reached an accuracy matching the experimental measurements. In addition, as decay amplitudes combine different form factors (in their canonical definition from $B \to K^*$ vector and tensor matrix elements), the absence of proper assessment of correlations among the different form factors can lead to a significant enhancement in the uncertainties of SM predictions of $B \to K^*$ decay amplitudes, and thus of the decay rate and its angular coefficients.

A fruitful approach to this problem has consisted in identifying observables built as suitable combinations of angular coefficients, where hadronic uncertainties cancel to a large extent (so-called form-factor independent or optimised observables). A guiding principle has been the use of effective theories (QCD factorisation/Soft Collinear Effective Theory at large recoil, Heavy Quark Effective Theory at low recoil) [29–31], allowing one to separate hard physics (occurring at scales around m_b) and soft physics (around and below $\Lambda_{\rm QCD}$) through an expansion of the form factors in Λ/m_b. The $B \to K^*$ decay amplitudes and related angular coefficients can be analysed through similar expansions, based on the factorisation of the seven QCD form factors in terms of only two soft form factors $\xi_\perp$ and $\xi_{||}$ [29, 32, 33]. In this context, form-factor-independent observables are defined

---

[1]Such a model would also have an impact on purely hadronic B and B_s decays. It could explain the tension in $\Delta A_{\rm CP}$ in $B \to \pi K$ decays and lead to a large enhancement above the SM expectations of the branching ratios of the purely isospin-violating decays $B_s \to \phi\pi$ and $B_s \to \phi\rho$ [10, 11]. The anomaly has also been addressed in the context of other NP models [8, 12–16] and within MFV [17].

as observables where the soft form factors cancel at leading order of the effective theory for the kinematic regime of interest (low or large K^* recoil). This has led for instance to the transverse asymmetries $A_T^{(i)}$ [4, 34–36] and later to the observables $P_i^{(\prime)}$ [3, 5] at large K^* recoil.[2] It was shown that a clever choice of observables could drastically reduce the sensitivity to hadronic inputs and enhance the sensitivity to New Physics [39].

Beyond leading order the above-mentioned decomposition of the seven QCD form factors in terms of two soft form factors receives α_s corrections (coming from hard-gluon exchanges) and $1/m_b$ power corrections (due to soft-gluon exchanges) [29, 33]. In the QCD factorisation analysis of $B \to K^*\mu^+\mu^-$ at large recoil [30], where amplitudes are expressed in terms of Wilson coefficients and soft form factors, these corrections to the relation between QCD and soft form factors manifest themselves as so-called *factorisable corrections*. The QCD factorisation analysis of the $B \to K^*\mu^+\mu^-$ amplitudes leads to further α_s and $1/m_b$ corrections called *non-factorisable corrections*, which are not related to form factors, for instance those coming from four-quark operators that can be inserted in the $B \to K^*\mu^+\mu^-$ decay (forming a $c\bar{c}$ pair decaying into a dimuon pair).

A first approach to predict $B \to K^*\mu^+\mu^-$ observables in the large-recoil region is naive factorisation, using the seven full (QCD) form factors for the three operators O_7 (electromagnetic), O_9 and O_{10} (semileptonic), but neglecting effects from four-quark operators beyond their high-energy contribution accounted for by the effective Wilson coefficients $C_{7,9}^{\mathrm{eff}}$ (see refs. [6, 40] for the definition of the operators and Wilson coefficients). If the form factors are computed fully non-perturbatively, predictions obtained in this way include *factorisable* α_s and $1/m_b$ power corrections to all orders. The method can be extended beyond naive factorisation by adding perturbative $\mathcal{O}(\alpha_s)$ corrections to the contribution from four-quark operators within the framework of QCD factorisation [30], as in ref. [6]. These corrections rely on the factorisation of matrix elements of hadronic operators at the leading power in a $(\Lambda/E_{K^*}, \Lambda/m_b)$ expansion. Contributions from four-quark operators at subleading power are not known and must be estimated. We will refer to these contributions as *non-factorisable power corrections*. As a downside of this approach, the form factor dependence does not cancel analytically in optimised observables, and in order to obtain accurate predictions it is crucial to know precisely the correlations among the uncertainties of the different form factors. In practice, however, LCSR results are usually presented without specifying the correlations among the various form factors. Moreover, while in principle parametric correlations originating from the hadronic inputs can be traced back easily, more sophisticated intrinsic correlations (e.g., the dependence on the Borel parameter) are hard to pin down.

A second approach consists in factorising the QCD form factors using effective field theory methods [29, 32, 33]. In this approach, correlations among the seven QCD form factors are to a large extent accounted for by their expression in terms of the two soft form factors $\xi_\perp$ and $\xi_\parallel$. At leading order in α_s (and at leading $1/m_b$ power) this leads to an analytic cancellation of form factors within optimised observables. Hence this method

---

[2]Similar observables can be built at low recoil [37–39], but the structure of the form-factor relations is different due to the different effective theory holding in this kinematic regime.

enables one to obtain precise predictions even in the absence of a precise knowledge on the correlations among the form factors. The dependence on form factors obviously reappears through (factorisable and non-factorisable) corrections to the leading-order results, either via (perturbative and calculable) $\mathcal{O}(\alpha_s)$- or (non-perturbative) $\mathcal{O}(\Lambda/m_b)$-corrections to the factorisation formula for QCD form factors. The fact that the dominant errors from form factors are suppressed in form-factor independent observables by one power of α_s or Λ/m_b makes these observables quite sensitive to subleading Λ/m_b power corrections (either factorisable or non-factorisable).

In order to determine the significance of the deviations in $B \to K^* \mu^+ \mu^-$ with respect to the Standard Model, it appears thus essential to estimate the size of the Λ/m_b power corrections. While an estimate of factorisable corrections is needed to get a reliable prediction from the second method, non-factorisable corrections have to be considered in both approaches. Non-factorisable power corrections cannot be computed from first principles, but factorisable ones can be extracted from QCD form factors by separating the contribution from soft form factors. This issue was discussed recently in ref. [41], suggesting that factorisable power corrections estimated in this way would imply substantial hadronic uncertainties on $B \to K^* \mu^+ \mu^-$ observables, much larger than what was found in other works. The present paper aims at reassessing these claims, showing that these large uncertainties are largely due to peculiar choices in the analysis method used in ref. [41] and are not a consequence of the theoretical information currently available on $B \to K^*$ form factors.

The paper is organized as follows. We begin in section 2 by describing the decomposition of QCD form factors in terms of soft form factors, including perturbative and power corrections, and discussing the role of the renormalisation scheme. In section 3 we describe our approach to factorisable power corrections, leading to our estimates for power correction parameters and their uncertainties. We then discuss the impact of these power corrections in the binned observables, and the scheme dependence. In section 4 we briefly discuss our approach to non-factorisable power corrections, which differs from the popular procedure [35] of multiplying each amplitude with a complex factor. In section 5 we present our final results for binned $B \to K^* \mu^+ \mu^-$ observables. We conclude in section 6. Appendix A addresses the issue of long-distance $c\bar{c}$ loops proposing different tests of the mechanism advocated in ref. [28] to explain the $B \to K^* \mu^+ \mu^-$ anomaly within the SM. A specific $B \to K^* \mu^+ \mu^-$ observable is discussed where the advocated charm-loop contribution cannot mimic New Physics below the J/ψ resonance, whereas two other tests are proposed to distinguish between SM long-distance effects and NP short-distance contributions. Appendix B summarises the factorisable perturbative corrections used in the renormalisation schemes considered for our study and appendix C collects SM predictions for other $B \to K^* \mu^+ \mu^-$ observables of interest.

2 Soft form factors

The evaluation of matrix elements for the decay $B \to K^* \mu^+ \mu^-$ involves seven non-perturbative form factors $V, A_{0,1,2}, T_{1,2,3}$ (see ref. [29] for definitions). LCSR calculations of these form factors suffer from large uncertainties originating from hadronic parameters,

and moreover rely on certain assumptions (modelling the continuum contribution, fixing the Borel parameter, etc.) introducing systematic uncertainties that are difficult to quantify. For a precise analysis of the decay $B \to K^* \mu^+ \mu^-$ it is thus desirable to reduce the sensitivity to the form factors as much as possible. To this end one can make use of the fact that in the symmetry limit of large K^* energies, i.e. for small invariant masses q^2 of the lepton pair, the seven QCD form factors $V, A_{0,1,2}, T_{1,2,3}$ reduce to two independent soft form factors $\xi_{\perp,\parallel}$, up to corrections of order $\mathcal{O}(\alpha_s)$ and $\mathcal{O}(\Lambda/m_b)$. A completely general parametrisation for the QCD form factors $V, A_{1,2,0}, T_{1,2,3}$ including all perturbative and non-perturbative corrections is given by

$$V(q^2) = \frac{m_B + m_{K^*}}{m_B} \xi_\perp(q^2) + \Delta V^{\alpha_s}(q^2) + \Delta V^\Lambda(q^2),$$

$$A_1(q^2) = \frac{2E}{m_B + m_{K^*}} \xi_\perp(q^2) + \Delta A_1^{\alpha_s}(q^2) + \Delta A_1^\Lambda(q^2),$$

$$A_2(q^2) = \frac{m_B}{m_B - m_{K^*}} \left[\xi_\perp(q^2) - \xi_\parallel(q^2)\right] + \Delta A_2^{\alpha_s}(q^2) + \Delta A_2^\Lambda(q^2),$$

$$A_0(q^2) = \frac{E}{m_{K^*}} \xi_\parallel(q^2) + \Delta A_0^{\alpha_s}(q^2) + \Delta A_0^\Lambda(q^2), \tag{2.1}$$

$$T_1(q^2) = \xi_\perp(q^2) + \Delta T_1^{\alpha_s}(q^2) + \Delta T_1^\Lambda(q^2),$$

$$T_2(q^2) = \frac{2E}{m_B} \xi_\perp(q^2) + \Delta T_2^{\alpha_s}(q^2) + \Delta T_2^\Lambda(q^2),$$

$$T_3(q^2) = \left[\xi_\perp(q^2) - \xi_\parallel(q^2)\right] + \Delta T_3^{\alpha_s}(q^2) + \Delta T_3^\Lambda(q^2),$$

with ΔF^{α_s} representing QCD corrections induced by hard gluons, and ΔF^Λ representing soft power corrections of order $\mathcal{O}(\Lambda/m_b)$. Even though these corrections are expected to be small compared to the current hadronic uncertainties of the QCD form factors, they play an important role in the study of optimised observables as they break the exact symmetry relations and therefore reintroduce a form factor dependence at order $\mathcal{O}(\alpha_s, \Lambda/m_b)$. While QCD corrections ΔF^{α_s} can be taken into account using results calculated within the framework of QCD factorisation [29], the inclusion of soft power corrections ΔF^Λ is not straightforward, since no first-principle calculation of these quantities exists.

On the other hand, LCSR determinations of the QCD form factors $V, A_{1,2,0}, T_{1,2,3}$ include all factorisable power corrections. Therefore as long as one is not interested in an explicit decomposition of the form factors into a soft contribution and power corrections, one can directly use the LCSR results as input for the form factors appearing in the naively factorised expressions for the amplitudes. In order to obtain precise predictions for observables involving QCD form factors, it is essential to assess properly all correlations among the errors of the different form factors within the LCSR calculation. The decomposition (2.1), on the other hand, if supplemented by a realistic estimate regarding the size of the $\mathcal{O}(\Lambda/m_b)$ corrections ΔF^Λ, takes into account the major part of correlations among the form factors by representing them in terms of the two soft form factors $\xi_{\perp,\parallel}$.

Therefore as long as the correlations among the LCSR form factors are not accessible *or* are not known to the same degree as they can be inferred from eq. (2.1), making use of the soft form factor decomposition is very convenient in order to obtain precise results for angular observables in the decay $B \to K^* \mu^+ \mu^-$.

The separation of the form factors $V, A_{1,2,0}, T_{1,2,3}$ into soft form factors $\xi_{\perp,\parallel}$ and perturbative/power corrections $\Delta F^{\alpha_s, \Lambda}$ in eq. (2.1) is not unique as one can always redefine $\xi_{\perp,\parallel}$ in such a way that these corrections are partly absorbed. In order to unambiguously define the soft form factors $\xi_{\perp,\parallel}$ (and thus the terms $\Delta F^{\alpha_s, \Lambda}$), one first has to fix a renormalisation scheme, i.e. define the $\xi_{\perp,\parallel}$ in terms of the physical form factors $V, A_{1,2,0}, T_{1,2,3}$.

A popular definition for $\xi_\perp$, used for example in refs. [6, 29, 39], is

$$\xi_\perp^{(1)}(q^2) \equiv \frac{m_B}{m_B + m_{K^*}} V(q^2). \tag{2.2}$$

where the superscript refers to the scheme thus defined. This definition eliminates all corrections to the form factor V leading to $\Delta V^{\alpha_s}(q^2) = \Delta V^\Lambda(q^2) = 0$. Alternatively one can define a second scheme for $\xi_\perp$, in terms of T_1,

$$\xi_\perp^{(2)}(q^2) \equiv T_1(q^2), \tag{2.3}$$

eliminating in this way $\Delta T_1^{\alpha_s}(q^2), \Delta T_1^\Lambda(q^2)$. This choice of scheme has been applied in refs. [41, 43], being quite convenient when extracting $T_1(0)$ from experimental data on $B \to K^* \gamma$. Note, however, that extracting $T_1(0)$ from $B \to K^* \gamma$ relies on the assumption that there is no new physics in the Wilson coefficients C_7 and C_7'. Furthermore, the $T_1^{\mathrm{exp}}(0)$ determined in this way can be identified with the form factor $T_1(0)$ only up to corrections of order $\mathcal{O}(\Lambda/m_b)$, stemming from four-quark operators (e.g., $c\bar{c}$ loops). These non-factorisable power corrections can neither be computed nor extracted from the QCD factorisation prediction for $B \to K^* \gamma$. Therefore, identifying $T_1^{\mathrm{exp}}(0)$ with $T_1(0)$ amounts to including unknown non-factorisable power corrections into T_1. Hence it cannot be used consistently as input in our approach to determine the factorisable $\mathcal{O}(\Lambda/m_b)$-corrections, and we will instead infer T_1 from LCSR calculations.

The soft form factor $\xi_\parallel$ can be defined as

$$\xi_\parallel^{(1)}(q^2) \equiv \frac{m_B + m_{K^*}}{2E} A_1(q^2) - \frac{m_B - m_{K^*}}{m_B} A_2(q^2), \tag{2.4}$$

as done for example in refs. [6, 39, 43]. This definition minimises power corrections in the form factors $A_{1,2}$ by correlating $\Delta A_1^{\alpha_s}(q^2), \Delta A_1^\Lambda(q^2)$ with $\Delta A_2^{\alpha_s}(q^2)$ and $\Delta A_2^\Lambda(q^2)$. An alternative scheme applied in ref. [29] is given by

$$\xi_\parallel^{(2)}(q^2) \equiv \frac{m_{K^*}}{E} A_0(q^2). \tag{2.5}$$

The choice of scheme determines which part of the $\mathcal{O}(\alpha_s, \Lambda/m_b)$ corrections will be absorbed into $\xi_{\perp,\parallel}$ and which part will remain in the functions $\Delta F^{\alpha_s, \Lambda}$. The perturbative corrections ΔF^{α_s} can be computed explicitly in each scheme, as illustrated in appendix B. If one had full control on the power corrections ΔF^Λ (including correlations among their

errors), physical quantities would not depend on the choice of scheme for the soft form factors at $\mathcal{O}(\alpha_s)$.[3] On the other hand, as long as information on the ΔF^Λ is not available or only available in part (for example because correlations cannot be assessed), predictions for observables will exhibit a scheme dependence at $\mathcal{O}(\Lambda/m_b)$. In this situation a proper choice of scheme can increase the precision of the theoretical prediction. Assume for example that a certain observable is dominated by the form factor V. Obviously a prediction employing scheme 1 for $\xi_\perp$ where V is directly taken as input will be more accurate in this case than a prediction relying on scheme 2 where V is obtained as a sum of T_1 and an unknown (or only partially known) power correction ΔV^Λ. This also depends on the relative size of the LCSR uncertainties in V and T_1. If T_1 is known much more precisely, and the total uncertainty in V is larger than expected power corrections, scheme 2 might be preferred in this case. The general statement is the following: different schemes lead to different uncertainties, and for each observable there is a preferred scheme where uncertainties are minimised.[4]

Different choices of the renormalisation scheme correspond to a reshuffling between soft form factors and power corrections. This choice affects the pattern of cancellation of power corrections when one considers clean observables. Indeed, since the soft form factors $\xi_{\perp,\|}$ cancel at leading order in clean observables, any power correction absorbed into the soft form factors according to the chosen renormalisation scheme will undergo a similar cancellation, so that it can contribute only at order $\mathcal{O}(\alpha_s, \Lambda/m_b) \times \mathcal{O}(\Lambda/m_b)$ (the second factor coming from the power correction itself). On the other hand, the power corrections that are kept explicitly in ΔF^Λ contribute at $\mathcal{O}(\Lambda/m_b)$ and their size must be assessed. Therefore the choice of the renormalisation scheme is crucial when one wants to determine how power corrections will affect clean observables.

In figure 1 we show the leading-power predictions for the observable S_5 [6], and the optimised observable P_5' [3] in two different schemes: $(\xi_\perp^{(1)}, \xi_\|^{(1)})$ defined from (V, A_1, A_2), and $(\xi_\perp^{(2)}, \xi_\|^{(2)})$ defined from (T_1, A_0). As input we have used the LCSR form factors from ref. [25]. The observable S_5 indeed exhibits the expected scheme dependence which can be considered as a measure of $\mathcal{O}(\Lambda/m_b)$ power corrections. The observable P_5', on the other hand, shows only a very mild scheme dependence because the soft form factors cancel at leading order pushing the scheme dependence to $\mathcal{O}(\alpha_s)$. In addition we show the prediction which one would obtain using uncorrelated QCD form factors without resorting to the soft form factor decomposition.

3 Factorisable power corrections

Even though no direct calculation of the factorisable power corrections ΔF^Λ exists, the fact that they are included in LCSR determinations of the QCD form factors allows for their estimation. One studies to which extend the full LCSR form factors violate the $(\Delta F^{\alpha_s}$-

---

[3]There is still a small residual scheme dependence at $\mathcal{O}(\Lambda/m_b)$ introduced by non-factorisable power corrections.

[4]Of course, for some observables different schemes might lead to very similar uncertainties; in these cases the choice of scheme has no impact.
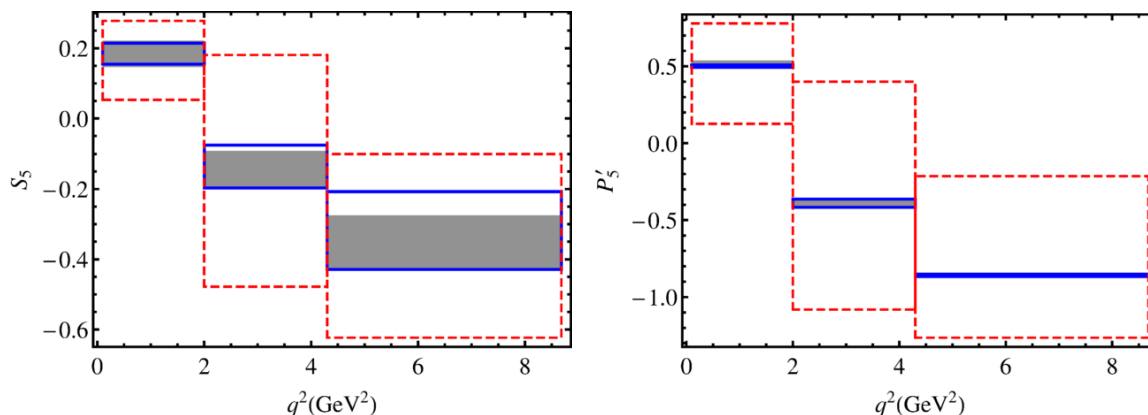
Figure 1. Scheme dependence in the prediction of the observables S_5 and P_5'. Power corrections are set to zero and uncertainties are solely due to form factors. Gray bands correspond to scheme 1 (V, A_1, A_2), blue (solid) boxes to scheme 2 (T_1, A_0), and red (dashed) boxes to the full-form-factor approach *with no correlations*. Form factor input is taken from ref. [25] in all cases.

corrected) symmetry relations (2.1) and attributes these deviations to the ΔF^Λ, which then can be determined from a fit. This basic strategy has been proposed and applied for the first time in ref. [41]. In our analysis we modify the approach of ref. [41] and go beyond it in several aspects. In the following we will specify our method in detail pointing out the differences with respect to ref. [41].

3.1 General approach

Following ref. [41] we parametrise the unknown soft power corrections ΔF^Λ as a polynomial in q^2/m_B^2,

$$\Delta F^\Lambda(q^2) = a_F + b_F \frac{q^2}{m_B^2} + c_F \frac{q^4}{m_B^4} + \ldots, \tag{3.1}$$

and perform a fit of the resulting form factor representation (2.1) to the QCD form factors from LCSR, using central values for the latter. In ref. [41] this fit was performed to first order in q^2/m_B^2 and the result $\hat{a}_F, \hat{b}_F$ was interpreted as an order-of-magnitude estimate for power corrections. Consequently the error associated to factorisable power corrections was estimated by varying independently $-|\hat{a}_F| \leq a_F \leq +|\hat{a}_F|$, $-|\hat{b}_F| \leq b_F \leq |\hat{b}_F|$ assuming the central values of ΔF^Λ to be zero. In our analysis we perform a fit to second order in q^2/m_B^2 and keep the correlated results $\hat{a}_F, \hat{b}_F, \hat{c}_F$ as (non-zero) central values for ΔF^Λ. With this procedure the central values of our predictions of observables will agree exactly with the ones which one would obtain in a calculation based on full LCSR form factors. In particular, they will not exhibit any dependence on the renormalisation scheme chosen for the soft form factors $\xi_{\perp,\parallel}$, apart from the one induced by non-factorisable power corrections.

For the error estimate we vary a_F, b_F, c_F symmetrically around their respective central values:

$$\begin{aligned} \hat{a}_F - \Delta\hat{a}_F &\leq a_F \leq \hat{a}_F + \Delta\hat{a}_F\,, \\ \hat{b}_F - \Delta\hat{b}_F &\leq b_F \leq \hat{b}_F + \Delta\hat{b}_F, \\ \hat{c}_F - \Delta\hat{c}_F &\leq c_F \leq \hat{c}_F + \Delta\hat{c}_F\,. \end{aligned} \tag{3.2}$$

	$\hat{a}_F^{(1)}$	$\hat{b}_F^{(1)}$	$\hat{c}_F^{(1)}$	$r(0\,\mathrm{GeV}^2)$	$r(4\,\mathrm{GeV}^2)$	$r(8\,\mathrm{GeV}^2)$
A_0(KMPW)	0.002 ± 0.000	0.590 ± 0.125	1.473 ± 0.251	0.007	0.220	0.333
A_0(BZ)	0.000 ± 0.000	0.003 ± 0.052	0.219 ± 0.121	0.002	0.012	0.032
A_1(KMPW)	-0.013 ± 0.025	-0.056 ± 0.018	0.158 ± 0.021	0.052	0.063	0.049
A_1(BZ)	-0.009 ± 0.027	0.042 ± 0.018	0.078 ± 0.017	0.032	0.003	0.029
A_2(KMPW)	-0.018 ± 0.023	-0.105 ± 0.022	0.192 ± 0.028	0.078	0.108	0.101
A_2(BZ)	-0.012 ± 0.024	0.037 ± 0.029	0.239 ± 0.034	0.050	0.006	0.053
T_1(KMPW)	-0.006 ± 0.031	-0.012 ± 0.054	-0.034 ± 0.095	0.016	0.018	0.020
T_1(BZ)	-0.024 ± 0.032	-0.019 ± 0.045	-0.014 ± 0.092	0.075	0.066	0.057
T_2(KMPW)	-0.005 ± 0.031	0.153 ± 0.043	0.544 ± 0.061	0.014	0.075	0.174
T_2(BZ)	-0.024 ± 0.031	0.040 ± 0.021	0.072 ± 0.019	0.074	0.046	0.015
T_3(KMPW)	-0.002 ± 0.022	0.308 ± 0.059	0.786 ± 0.093	0.007	0.181	0.322
T_3(BZ)	-0.035 ± 0.019	-0.021 ± 0.021	0.097 ± 0.025	0.178	0.154	0.116

Table 1. Fit results for the power-correction parameters in the case of scheme 1 –with $(\xi_\perp^{(1)}, \xi_\parallel^{(1)})$ defined from (V, A_1, A_2). The relative size $r(q^2)$ is also shown for $q^2 = 0\,\mathrm{GeV}^2, 4\,\mathrm{GeV}^2, 8\,\mathrm{GeV}^2$. The label KMPW refers to LCSR input from ref. [25], and BZ to ref. [44]. In this scheme, V receives no power corrections and therefore the corresponding parameters vanish.

In principle the errors $\Delta\hat{a}_F, \Delta\hat{b}_F, \Delta\hat{c}_F$ are related to the errors of the QCD form factors and could be determined from a fit if the correlations among the form factors were known precisely. In the absence of such knowledge one is forced to rely on dimensional arguments, exploiting the Λ/m_b suppression of the ΔF^Λ. To this end we consider an expanded approximation $F(q^2) = A_F + B_F q^2/m_B^2 + C_F q^4/m_B^4$ of the full LCSR form factors and attribute a 10% error to the power corrections setting $\Delta\hat{a}_F = 0.1A_F, \Delta\hat{b}_F = 0.1B_F, \Delta\hat{c}_F = 0.1C_F.$[5] Given the fact that $\Delta F^\Lambda \sim F \times \mathcal{O}(\Lambda/m_b) \sim 0.1F$ this amounts to assigning an error of $\sim 100\%$ to the result $\Delta\hat{F}$ from the fit.

Note that with our approach any future improvement on the precision of form factor calculations can be accounted for by reducing the size of the free parameters $\Delta\hat{a}_F, \Delta\hat{b}_F, \Delta\hat{c}_F$ accordingly. On the contrary, in the method of ref. [41] the errors are frozen due to their determination from central values, and they do not approach zero in the hypothetical limit of exact knowledge of the form factors, if (as expected) they do not fulfill exactly the leading power symmetry relations.

The soft form factor decomposition (2.1) is not unique and depends on the renormalisation scheme for the soft form factors $\xi_\perp, \xi_\parallel$. In the following section 3.2 we will discuss how the choice of scheme affects the errors induced by power corrections for $B \to K^* \mu^+ \mu^-$ angular observables.

In tables 1 and 2 we show respectively our fit results in the two different schemes, with $(\xi_\perp^{(1)}, \xi_\parallel^{(1)})$ defined from (V, A_1, A_2) and with $(\xi_\perp^{(2)}, \xi_\parallel^{(2)})$ defined from (T_1, A_0), and for two different sets of LCSR form factors [25, 44]. Apart from the actual values of the coefficients

---

[5]The expanded approximation is only used to obtain a normalisation for the errors $\Delta\hat{a}_F, \Delta\hat{b}_F, \Delta\hat{c}_F$, while everywhere else in our analysis the full q^2-dependence of the form factors is used.

	$\hat{a}_F^{(2)}$	$\hat{b}_F^{(2)}$	$\hat{c}_F^{(2)}$	$r(0\,\mathrm{GeV}^2)$	$r(4\,\mathrm{GeV}^2)$	$r(8\,\mathrm{GeV}^2)$
V(KMPW)	0.005 ± 0.036	0.013 ± 0.063	0.039 ± 0.113	0.016	0.018	0.020
V(BZ)	0.027 ± 0.039	0.021 ± 0.053	0.014 ± 0.107	0.072	0.064	0.056
A_1(KMPW)	-0.009 ± 0.025	-0.049 ± 0.018	0.166 ± 0.021	0.035	0.043	0.027
A_1(BZ)	0.011 ± 0.027	0.038 ± 0.018	0.069 ± 0.017	0.043	0.061	0.083
A_2(KMPW)	-0.010 ± 0.023	0.099 ± 0.022	1.496 ± 0.028	0.040	0.135	0.451
A_2(BZ)	0.017 ± 0.024	0.055 ± 0.029	0.400 ± 0.034	0.071	0.115	0.187
T_2(KMPW)	0.000 ± 0.000	0.161 ± 0.043	0.553 ± 0.061	0.002	0.092	0.191
T_2(BZ)	0.000 ± 0.000	0.035 ± 0.021	0.062 ± 0.019	0.000	0.019	0.040
T_3(KMPW)	0.005 ± 0.022	0.486 ± 0.059	1.895 ± 0.093	0.026	0.352	0.639
T_3(BZ)	-0.011 ± 0.019	-0.006 ± 0.021	0.235 ± 0.025	0.054	0.028	0.027

Table 2. Fit results for the power-correction parameters in the case of scheme 2 –with $(\xi_\perp^{(2)}, \xi_\parallel^{(2)})$ defined from (T_1, A_0). The relative size $r(q^2)$ is also shown for $q^2 = 0\,\mathrm{GeV}^2, 4\,\mathrm{GeV}^2, 8\,\mathrm{GeV}^2$. The label KMPW refers to LCSR input from ref. [25], and BZ to ref. [44]. In this scheme, A_0 and T_1 receive no power corrections and therefore the corresponding parameters vanish.

$\hat{a}_F$, $\hat{b}_F$, $\hat{c}_F$ and the estimated errors, we also display the relative size

$$r(q^2) = \left| \frac{\hat{a}_F + \hat{b}_F \frac{q^2}{m_B^2} + \hat{c}_F \frac{q^4}{m_B^4}}{F(q^2)} \right| \tag{3.3}$$

for different invariant masses $q^2 = 0\,\mathrm{GeV}^2, 4\,\mathrm{GeV}^2, 8\,\mathrm{GeV}^2$ of the lepton pair. The results confirm that power corrections are typically $\lesssim 10\%$ for $q^2 \leq 4\,\mathrm{GeV}^2$ as expected from dimensional arguments. In the case of LCSR input from ref. [25] (KMPW) slightly larger power corrections are found for larger values of q^2 for the form factor T_3, as well as for A_0 in scheme 1 (A_2 in scheme 2). However, this is not problematic in the case of the $B \to K^* \mu^+ \mu^-$ transversity amplitudes, given that A_0 is suppressed by powers of the lepton mass and T_3 is relatively subdominant as compared to other tensor contributions due to their relative kinematic prefactors at large recoil [39].

3.2 Correlations of power corrections

The quantities a_F, b_F, c_F parametrising the factorisable power corrections are subject to several constraints, resulting from (a) kinematic correlations among QCD form factors at maximum recoil, and (b) the definition of the soft form factors $\xi_\perp$ and $\xi_\parallel$. Taking into account these correlations reduces the number of parameters to be varied in the error analysis, reducing correspondingly the overall uncertainties in the observables. Not taking into account such correlations would lead to an over-estimation of the effect of factorisable power corrections.

At $q^2 = 0$ the QCD form factors obey the exact equations[6]

$$A_0(0) = \frac{m_B + m_{K^*}}{2m_{K^*}} A_1(0) - \frac{m_B - m_{K^*}}{2m_{K^*}} A_2(0),$$

$$T_1(0) = T_2(0). \tag{3.4}$$

---

[6]The relation between A_0, A_1 and A_2 is only approximately fulfilled for the input from LCSR determinations. In practice we enforce it to hold exactly by a rescaling of A_0.

These equations imply that the soft power corrections fulfil

$$a_{A_0} = \frac{m_B + m_{K^*}}{2m_{K^*}} a_{A_1} - \frac{m_B - m_{K^*}}{2m_{K^*}} a_{A_2} \,,$$

$$a_{T_1} = a_{T_2} \,. \tag{3.5}$$

While the correlations of eq. (3.5) always apply, additional constraints depend on the renormalisation scheme chosen for $\xi_\perp$ and $\xi_\parallel$. Defining $\xi_\perp$ in terms of V according to eq. (2.2) results in

$$a_V^{(1)} = 0, \qquad b_V^{(1)} = 0, \qquad c_V^{(1)} = 0, \tag{3.6}$$

while a definition from T_1 following eq. (2.3) gives

$$a_{T_1}^{(2)} = 0, \qquad b_{T_1}^{(2)} = 0, \qquad c_{T_1}^{(2)} = 0. \tag{3.7}$$

If the soft form factor $\xi_\parallel$ is defined from $A_{1,2}$ in eq. (2.4), one finds the correlations

$$a_{A_2}^{(1)} = \frac{m_B + m_{K^*}}{m_B - m_{K^*}} a_{A_1}^{(1)},$$

$$b_{A_2}^{(1)} = \frac{m_B + m_{K^*}}{m_B - m_{K^*}} \left[a_{A_1}^{(1)} + b_{A_1}^{(1)} \right]$$

$$c_{A_2}^{(1)} = \frac{m_B + m_{K^*}}{m_B - m_{K^*}} \left[a_{A_1}^{(1)} + b_{A_1}^{(1)} + c_{A_1}^{(1)} \right] \tag{3.8}$$

for the corresponding power corrections. The definition (2.5) in terms of A_0, on the other hand, translates into

$$a_{A_0}^{(2)} = 0, \qquad b_{A_0}^{(2)} = 0, \qquad c_{A_0}^{(2)} = 0. \tag{3.9}$$

Note that unlike the authors of ref. [41], we do not enforce any of the constraints (either the general constraints eqs. (3.4)–(3.5) or the renormalisation-scheme dependent ones eqs. (3.6)–(3.8)) in the fit for the central values $\hat{a}_F, \hat{b}_F, \hat{c}_F$. Our results from the fit given in tables 1 and 2 respect the constraints within the overall accuracy of the fit, limited by the parametrisation of the power correction functions as second order polynomials. The precision to which the correlations are fulfilled can be improved by adding higher-order coefficients $d_F, e_F, \ldots$ in the fit.[7]

For the estimation of errors associated to power corrections, we vary the parameters a_F, b_F, c_F within the ranges specified in tables 1 and 2, imposing in addition the constraints (3.5)–(3.9) according to the respective scheme. As the correlations depend on the definition chosen for the soft form factors $\xi_{\perp,\parallel}$, the errors originating from factorisable power corrections are scheme dependent. In figure 2 we show the corresponding errors

---

[7]Imposing the correlations in the fit by hand would not improve the overall accuracy of the fit result. As constraints are mostly related to the endpoint $q^2 = 0$, it would imply that form factor values $F(0)$ at $q^2 = 0$ have a larger weight in the fit than $F(q^2)$ at larger q^2. The resulting functions for the sum of soft form factors and power corrections would describe then the full form factors better at $q^2 \approx 0$, but worse in the physically more interesting region $q^2 > 1\,\mathrm{GeV}^2$.
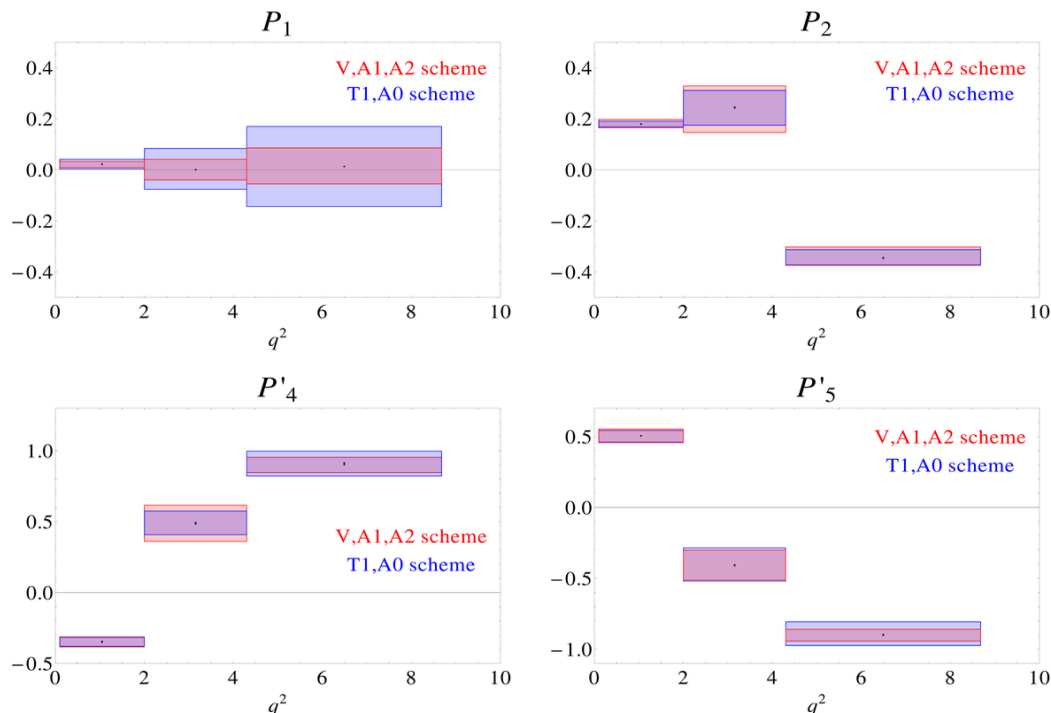
Figure 2. Scheme dependence on the prediction of the observables P_1, P_2, P_4', P_5' in QCD factorisation. These results include factorisable power corrections as described in the text.

for the observables P_1, P_2, P_4' and P_5' in the two schemes, with $(\xi_\perp^{(1)}, \xi_\parallel^{(1)})$ defined from (V, A_1, A_2) and with $(\xi_\perp^{(2)}, \xi_\parallel^{(2)})$ defined from (T_1, A_0).[8] As input we have used the LCSR form factors from ref. [25]. For $q^2 > 4\,\text{GeV}^2$, the observables P_1 and P_5' exhibit significantly smaller errors in the first scheme, while the observables P_2 and P_4' have slightly smaller uncertainties in the second scheme.

The scheme dependence of the observables is dominated by the definition of $\xi_\perp$. The fact that the Wilson coefficient C_9 always enters in combination with a vector form factor V, A_1, A_2, while C_7 enters in combination with a tensor form factor $T_{1,2,3}$, thus explains that observables with a high sensitivity to C_9 like the third bin of P_5' can be predicted more precisely in the first scheme, while observables with a higher sensitivity to C_7 like P_2 are better described in the second. Concerning $\xi_\parallel$, the situation is unambiguous: since any contribution of the form factor A_0 to physical observables is always suppressed by small lepton masses, the constraint (3.9) does not improve the precision of the theory predictions in contrast to the correlation (3.8) obtained in the first scheme. On the other hand, one may think that the first scheme has the disadvantage of $\xi_\parallel$ being built from two form factors $A_{1,2}$, which would lead to an increase of the error on $\xi_\parallel$ if one takes the errors on $A_{1,2}$ as independent. This problem can actually be avoided because eq. (3.4) allows us to extract the error on $\xi_\parallel(0)$ from $A_0(0)$.[9]

---

[8]Obviously, these two examples are not limitative: other pairings of normalisation schemes could be considered, and additional schemes could be devised.

[9]We increase the error on $\xi_\parallel(0)$ obtained in this way by the small extent to which the LCSR form factors

In ref. [41] the authors have chosen a scheme similar to our second scheme, by defining $\xi_\perp$ and $\xi_\parallel$ in terms of T_1 and A_0. As discussed above, this explains to some extent the big uncertainties they find in the observable P_5'. Their scheme differs, however, from our second scheme as they assigned an ad-hoc q^2-dependence to the soft form factors $\xi_{\perp,\parallel}$ which differs from that of the QCD form factors T_1, A_0: equations (2.3) and (2.5) are thus fulfilled only at $q^2 = 0$. As a consequence, only the a-coefficients are correlated in their scheme, and the correlations of b- and higher-order coefficients are lost. This reduces the number of correlations artificially from eight, as in our second scheme, to only four in their scheme (if parameters a,b,c are considered). Another difference in their study is that they extract T_1 from experimental data on $B \to K^* \gamma$ while we take T_1 from its LCSR calculations — the limits of the first approach compared to our extraction from theoretical computations of the form factors have already been discussed in a previous section, after eq. (2.3). Concerning the extraction of factorisable power corrections, our main differences with respect to the approach in ref. [41] are the following: we vary the power correction parameters a, b, c around their (non-zero) fit values with a separate assessment of the uncertainties ($\hat{a}_F - \Delta\hat{a}_F \leq a_F \leq \hat{a}_F \leq \Delta\hat{a}_F$), rather than varying them in the whole range given by the magnitude of the fit value ($-|\hat{a}_F| \leq a_F \leq |\hat{a}_F|$). We have chosen a different renormalization scheme leading to stronger correlations and generally smaller errors. Furthermore, we do not average different form factor determinations (especially we do not perform average of absolute values, leading to numerical values for the power correction parameters inconsistent with respect to the renormalisation scheme chosen). These differences result in better controlled uncertainties on the angular observables shown in figure 2.

4 Non-factorisable power corrections

Even in the situation in which QCD form factors were known exactly, the problem of non-factorisable contributions would persist. This problem is related to the factorisation of hadronic contributions to $B \to K^* \mu^+ \mu^-$ from four-quark and chromo-magnetic operators where the lepton pair is produced via a virtual photon. At large recoil, the factorisation of the corresponding matrix elements into form factors, light-cone distribution amplitudes and hard-scattering kernels is a formal prediction of SCET/QCD factorisation at leading power in the $1/m_b$ expansion [30]. At subleading power, however, new unknown non-perturbative contributions would appear. These power corrections are called non-factorisable, and appear irrespectively of whether QCD form factors are expressed in terms of soft form factors or not. An estimate of such power corrections must be included in the predictions.

An approach that has become popular [35] consists in parametrising both factorisable and non-factorisable power corrections jointly via a set of complex factors multiplying

---

violate the relation (3.4). For the form factors from ref. [25] we are still left with determining the error for the slope-parameter of the q^2-dependence of $\xi_\parallel$ from A_1 and A_2. Even though the error of $\xi_\parallel$ increases significantly for large q^2 because of the unknown correlation of uncertainties in the slopes of A_1 and A_2, this has only a minor impact on the errors of optimised observables where the form-factor enters only at next-to-leading order.

each transversity amplitude, with typical absolute values of order 10% (motivated from dimensional arguments) and arbitrary phases.[10] Even if this ad-hoc procedure tends to underestimate the errors associated to individual transversity amplitudes in the vicinity of the zeroes, this is not the case for observables. Error estimates based on this strategy are expected to give reasonable results for physical observables because they receive contributions from various amplitudes, and left- and right-handed transversity amplitudes do not vanish at the same value of q^2 (with the sets of form factors currently available).

In our present analysis we could use the same technique for non-factorisable power corrections alone (since factorisable power corrections are estimated separately using the more sophisticated methods described in section 3), but that would clearly overestimate the effect. Note that the contributions from electromagnetic and semileptonic operators are free from non-factorisable corrections, so that the terms proportional to $C_{7,9,10}^{(\prime)}$, which are leading contributions, must not be inflated artificially.

Therefore we proceed as follows: in ref. [30], the amplitudes of $\langle K^*\gamma^*|H_{\text{eff}}|B\rangle$ are decomposed in terms of three hadronic form factors $\mathcal{T}_i(q^2)$, which are re-expressed in terms of Wilson coefficients, soft form factors, light-cone sum rules and hard-scattering kernels using QCD factorisation. In each of the amplitudes, we single out the part involving the hadronic form factors $\mathcal{T}_i^{\text{had}}$, obtained from the functions $\mathcal{T}_i$ by [11] $\mathcal{T}_i^{\text{had}} = \mathcal{T}_i|_{C_7^{(\prime)} \to 0}$. Finally, we multiply each of these amplitudes with a complex q^2-dependent factor:

$$\mathcal{T}_i^{\text{had}} \to \left(1 + r_i(q^2)\right)\mathcal{T}_i^{\text{had}}, \tag{4.1}$$

with

$$r_i(s) = r_i^a e^{i\phi_i^a} + r_i^b e^{i\phi_i^b}(s/m_B^2) + r_i^c e^{i\phi_i^c}(s/m_B^2)^2. \tag{4.2}$$

Let us note at this point that the relationship $\mathcal{T}_2 = 2E/m_B \, \mathcal{T}_1$ [30] does not hold at subleading power, so that our parameters r_2 and r_3 for non-factorisable power corrections are unrelated.

We define our central values as the ones with $r_i(q^2) \equiv 0$, and estimate the uncertainties from non-factorisable power corrections by varying $r_i^{a,b,c} \in [0, 0.1]$ and $\phi_i^{a,b,c} \in [-\pi, \pi]$ independently, corresponding to a $\sim 10\%$ correction with an arbitrary phase. The uncertainties for each observable are then obtained by performing a random scan and taking the maximum deviation from the central values to each side, to obtain (possibly asymmetric) upward and downward error bars.

5 Results

5.1 SM predictions for angular observables

In this section we present the set of SM predictions for the various angular observables. We give results within scheme 1 (where soft form factors are defined from V, A_1, A_2),

---

[10]Shortcomings related to this procedure, as well as the general problems related to the estimation of power corrections in $B \to K^*\ell\ell$ have been recently reviewed in ref. [17].

[11]The amplitudes $\mathcal{T}_i$ are defined from $\langle K^*\gamma^*|H_{\text{eff}}|B\rangle$ and thus do not contain contributions proportional to $C_{9,10}^{(\prime)}$. In the presence of right-handed currents (i.e., chirally-flipped operators $\mathcal{O}_i'$) the set of amplitudes generalizes to $\mathcal{T}_i^{\pm}$ (see e.g., ref. [45]). Here we use the collective symbol $\mathcal{T}_i$ for all of them.

which globally leads to smaller uncertainties related to factorisable power corrections, as detailed in section 3.2. We do not provide the results for scheme 2 (where soft form factors are defined from T_1, A_0), but we do include these in the plots below (figure 3) for comparison. We have explored several schemes[12] and find that scheme 1 is preferred for many observables. In the case of observables sensitive to C_9, of particular interest for the analysis of the deviations observed by LHCb [7], an argument in favour of this scheme has been given in section 3.2. We stress that in principle one can choose different schemes for different observables consistently, allowing one to optimise the accuracy of the theory prediction for each individual observables. In global analyses (i.e. global fits), on the other hand, all observables should be calculated using the same scheme because otherwise different observables would depend on different sets of theory parameters $\xi_{\perp,\parallel}^{(i)}$ and $a_F^{(i)}, b_F^{(i)}, c_F^{(i)}$ and correlations among the predictions for different observables would be lost.

The central value for each observable corresponds to the value obtained by setting all the parameters to their central values, including factorisable power corrections, as obtained from the central values of the parameters a_F, b_F, c_F in tables 1 and 2. This is an important difference with respect to previous analyses based on QCD factorisation, where central values correspond to subleading contributions put to zero. In particular our central values are comparable to those obtained from analyses that use QCD form factors (e.g., ref. [6]).

Uncertainties related to factorisable and non-factorisable power corrections are computed as described in sections 3 and 4, and presented separately. The rest of the error analysis is separated into "parametric" and "form factors". The first accounts for the variation of all input parameters except form factors (masses, decay constants, Gegenbauer moments, renormalisation scale, taking the same inputs as in ref. [39]), and the second for the errors associated to $\xi_{\parallel,\perp}(q^2)$, inherited from the form factor input in the respective scheme. For all four types of uncertainties, errors ranges are obtained in the same way, which we illustrate by focusing on the parametric uncertainties: we make a random flat scan of all relevant parameters (masses, etc.) simultaneously, within the range given by their "uncertainty" (error bars given by the PDG [42] in the case of masses, the renormalisation scale between $m_b/2$ and $2m_b$, etc.), while keeping the other sets of parameters (form factors, power corrections) fixed to their central values. We compute each observable for every point in the scan, and take the corresponding maximum and minimum value. Upward and downward error bars are then obtained by comparing the extreme values with the central values.

Table 3 contains our results for a selected set of observables in scheme 1, where we give both results based on form-factor input from [25] (KMPW) and [44] (BZ). The corresponding predictions for other observables are collected for reference in appendix C. We note that for optimised observables and for input taken from KMPW, parametric uncertainties, form factor uncertainties and uncertainties from factorisable power corrections are usually of the same order of magnitude, while uncertainties from non-factorisable power

---

[12]Besides schemes 1 and 2 discussed in the paper, we have also considered a mixed scheme were soft form factors are defined from V, A_0. This scheme leads to very similar results to scheme 2.

Observable	KMPW - scheme 1	BZ - scheme 1
$\langle P_1 \rangle_{[0.1,2]}$	$0.021^{+0.004+0.008+0.011+0.034}_{-0.003-0.010-0.012-0.043}$	$0.035^{+0.005+0.000+0.010+0.035}_{-0.003-0.000-0.011-0.045}$
$\langle P_1 \rangle_{[2,4.3]}$	$0.000^{+0.004+0.001+0.040+0.009}_{-0.002-0.006-0.040-0.013}$	$-0.023^{+0.003+0.000+0.049+0.007}_{-0.003-0.000-0.057-0.009}$
$\langle P_1 \rangle_{[4.3,8.68]}$	$0.013^{+0.002+0.046+0.071+0.005}_{-0.001-0.037-0.069-0.005}$	$-0.101^{+0.002+0.000+0.076+0.005}_{-0.003-0.000-0.074-0.005}$
$\langle P_1 \rangle_{[1,6]}$	$0.009^{+0.002+0.009+0.037+0.010}_{-0.001-0.012-0.040-0.014}$	$-0.031^{+0.003+0.000+0.045+0.009}_{-0.004-0.000-0.054-0.011}$
$\langle P_1 \rangle_{[1,2]}$	$0.002^{+0.003+0.015+0.020+0.033}_{-0.002-0.020-0.023-0.043}$	$0.031^{+0.004+0.000+0.015+0.033}_{-0.003-0.000-0.019-0.043}$
$\langle P_1 \rangle_{[4.3,6]}$	$0.021^{+0.004+0.039+0.068+0.002}_{-0.002-0.033-0.069-0.002}$	$-0.071^{+0.000+0.000+0.077+0.003}_{-0.002-0.000-0.077-0.003}$
$\langle P_1 \rangle_{[6,8]}$	$0.015^{+0.003+0.049+0.073+0.004}_{-0.001-0.039-0.070-0.004}$	$-0.104^{+0.002+0.000+0.077+0.004}_{-0.003-0.000-0.075-0.005}$
$\langle P_2 \rangle_{[0.1,2]}$	$0.179^{+0.008+0.006+0.018+0.002}_{-0.007-0.007-0.015-0.002}$	$0.187^{+0.008+0.000+0.015+0.002}_{-0.008-0.000-0.016-0.002}$
$\langle P_2 \rangle_{[2,4.3]}$	$0.244^{+0.030+0.044+0.083+0.010}_{-0.053-0.038-0.098-0.013}$	$0.156^{+0.035+0.000+0.102+0.011}_{-0.056-0.000-0.099-0.015}$
$\langle P_2 \rangle_{[4.3,8.68]}$	$-0.344^{+0.028+0.030+0.041+0.004}_{-0.050-0.019-0.030-0.003}$	$-0.386^{+0.021+0.000+0.032+0.003}_{-0.039-0.000-0.022-0.002}$
$\langle P_2 \rangle_{[1,6]}$	$0.106^{+0.026+0.042+0.071+0.008}_{-0.054-0.034-0.078-0.010}$	$0.034^{+0.026+0.000+0.082+0.008}_{-0.052-0.000-0.076-0.011}$
$\langle P_2 \rangle_{[1,2]}$	$0.409^{+0.017+0.012+0.030+0.004}_{-0.017-0.016-0.031-0.004}$	$0.429^{+0.015+0.000+0.022+0.004}_{-0.016-0.000-0.031-0.004}$
$\langle P_2 \rangle_{[4.3,6]}$	$-0.210^{+0.030+0.044+0.073+0.006}_{-0.066-0.031-0.057-0.007}$	$-0.281^{+0.023+0.000+0.063+0.005}_{-0.054-0.000-0.045-0.006}$
$\langle P_2 \rangle_{[6,8]}$	$-0.376^{+0.026+0.025+0.034+0.003}_{-0.057-0.016-0.024-0.002}$	$-0.412^{+0.019+0.000+0.025+0.003}_{-0.043-0.000-0.016-0.002}$
$\langle P_4' \rangle_{[0.1,2]}$	$-0.352^{+0.019+0.047+0.039+0.009}_{-0.016-0.031-0.031-0.009}$	$-0.316^{+0.024+0.001+0.042+0.010}_{-0.017-0.001-0.034-0.010}$
$\langle P_4' \rangle_{[2,4.3]}$	$0.485^{+0.047+0.082+0.129+0.010}_{-0.039-0.094-0.125-0.009}$	$0.628^{+0.041+0.001+0.112+0.010}_{-0.036-0.002-0.131-0.009}$
$\langle P_4' \rangle_{[4.3,8.68]}$	$0.902^{+0.014+0.045+0.050+0.005}_{-0.008-0.060-0.056-0.004}$	$0.993^{+0.010+0.000+0.043+0.004}_{-0.005-0.000-0.049-0.003}$
$\langle P_4' \rangle_{[1,6]}$	$0.476^{+0.041+0.091+0.116+0.009}_{-0.034-0.095-0.111-0.008}$	$0.594^{+0.037+0.002+0.103+0.009}_{-0.031-0.002-0.117-0.008}$
$\langle P_4' \rangle_{[1,2]}$	$-0.186^{+0.034+0.059+0.091+0.011}_{-0.023-0.053-0.069-0.011}$	$-0.105^{+0.044+0.002+0.095+0.012}_{-0.028-0.002-0.080-0.012}$
$\langle P_4' \rangle_{[4.3,6]}$	$0.842^{+0.018+0.052+0.067+0.004}_{-0.015-0.069-0.076-0.004}$	$0.950^{+0.012+0.000+0.054+0.003}_{-0.010-0.000-0.067-0.003}$
$\langle P_4' \rangle_{[6,8]}$	$0.930^{+0.012+0.038+0.046+0.005}_{-0.011-0.053-0.052-0.004}$	$1.019^{+0.008+0.000+0.040+0.004}_{-0.009-0.000-0.044-0.003}$
$\langle P_5' \rangle_{[0.1,2]}$	$0.505^{+0.015+0.014+0.045+0.011}_{-0.024-0.024-0.049-0.012}$	$0.506^{+0.016+0.000+0.042+0.012}_{-0.025-0.000-0.048-0.013}$
$\langle P_5' \rangle_{[2,4.3]}$	$-0.411^{+0.050+0.017+0.109+0.016}_{-0.072-0.015-0.101-0.020}$	$-0.436^{+0.048+0.000+0.095+0.016}_{-0.068-0.000-0.097-0.019}$
$\langle P_5' \rangle_{[4.3,8.68]}$	$-0.902^{+0.025+0.019+0.043+0.006}_{-0.043-0.021-0.041-0.006}$	$-0.853^{+0.021+0.000+0.048+0.006}_{-0.036-0.000-0.047-0.006}$
$\langle P_5' \rangle_{[1,6]}$	$-0.412^{+0.042+0.026+0.096+0.014}_{-0.070-0.045-0.089-0.017}$	$-0.416^{+0.039+0.000+0.083+0.014}_{-0.064-0.000-0.086-0.017}$
$\langle P_5' \rangle_{[1,2]}$	$0.331^{+0.029+0.013+0.074+0.015}_{-0.045-0.006-0.081-0.017}$	$0.315^{+0.032+0.001+0.073+0.016}_{-0.048-0.001-0.084-0.018}$
$\langle P_5' \rangle_{[4.3,6]}$	$-0.832^{+0.027+0.018+0.058+0.007}_{-0.060-0.013-0.057-0.007}$	$-0.802^{+0.024+0.000+0.059+0.006}_{-0.052-0.000-0.059-0.007}$
$\langle P_5' \rangle_{[6,8]}$	$-0.934^{+0.024+0.021+0.039+0.005}_{-0.047-0.022-0.038-0.005}$	$-0.880^{+0.020+0.000+0.045+0.005}_{-0.039-0.000-0.044-0.005}$

Table 3. SM predictions for the observables P_1, P_2, P_4', P_5' in various bins, computed in scheme 1, where the soft form factors are determined from (V, A_1, A_2). First error is parametric, second is form factors, third is factorisable power corrections and fourth is non-factorisable power corrections. The first column (KMPW) is obtained with LCSR input from ref. [25] and the second one (BZ) from ref. [44]. Slight differences in the central values with respect to refs. [7, 39] are due to a different numerical value for the charm pole mass, which we take here as $m_c = 1.47 \pm 0.20\,\mathrm{GeV}$.
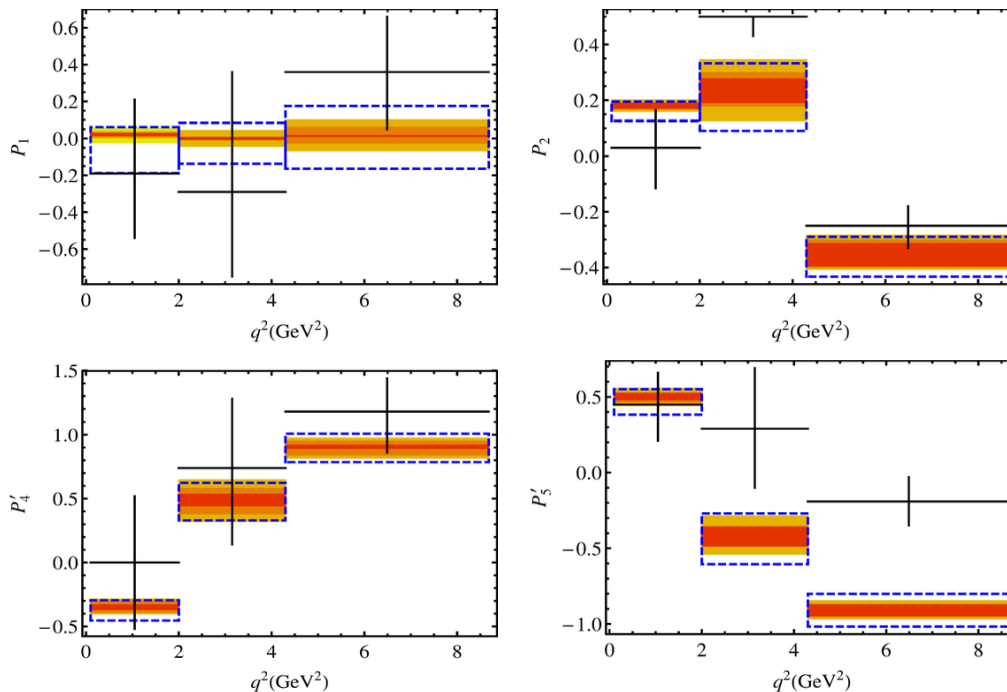
Figure 3. SM predictions for the observables P_1, P_2, P_4', P_5' obtained as described in the text. The bands correspond, from darker to lighter, to uncertainties from parametric, form factor, factorisable and non-factorisable power corrections, added sequentially in quadrature. The data points correspond to experimental data from LHCb [1, 2]. Blue dashed boxes are predictions in scheme 2.

corrections are typically smaller. For "non-optimised observables" uncertainties are dominated by the form factor input as expected. For input taken from BZ, the uncertainties stemming from the form factors are generally smaller, in particular they are completely negligible for optimised observables. In figure 3 we illustrate the predictions corresponding to table 3 in the case of KMPW form factors, together with the experimental data points from the LHCb analyses of refs. [1, 2]. In these figures we add sequentially and quadratically the four different sets of uncertainties as in table 3. We include also the predictions in scheme 2 for comparison, noting that they generally lead to larger uncertainties in P_1, P_2, P_4', P_5'.

5.2 Impact of $c\bar{c}$ loops

Our computation includes contributions from $c\bar{c}$ loops, through factorisable contributions as well as non-factorisable contributions with hard-gluon exchanges. As already mentioned in the introduction, the size of the remaining long-distance contribution from $c\bar{c}$ loops is a debated issue, with some contributions considered in ref. [25] for $B \to K^*\mu\mu$ and further work (unfortunately only for $B \to K\mu\mu$) in ref. [53]. We have not considered these contributions up to now explicitly, even though they are partly encoded in the power corrections discussed in the previous sections. Indeed, these contributions do not stand on the same footing as the factorisable power corrections discussed in section 3. While we

presented a systematic procedure to estimate the size in the latter case, here we can only rely on a partial computation existing in the literature [25].

In ref. [25] the soft-gluon contribution originating from the insertion of 4-quark operators $\mathcal{O}_{1,2}^c$ and penguin operators $\mathcal{O}_{3-6}$ induces a positive contribution inside C_9^{eff}. For an overall estimate of non-perturbative contributions from hadronic operators, we take the terms ΔC_9 in ref. [25], which include the LO perturbative contribution from $O_{1,2}$ together with non-factorisable soft-gluon emission from the charm loop. In order to separate the long-distance contribution, we subtract the perturbative contribution from ΔC_9 (using eq. (7.14) and table 2 of ref. [25]), to obtain the (three) functions $\tilde{g}(q^2)$ according to eq. (5.6) of ref. [25]. The results should match well the functions $\tilde{g}$, at least below $4\,\text{GeV}^2$, computed for $m_c = 1.05\,\text{GeV}$. In order to gauge the possible shift in our central values (computed at the reference value $m_c = 1.47\,\text{GeV}$), we shift $\tilde{g}$ by -35% as indicated in table 1 of ref. [25]. This gives three ranges of variations (one for each function $\tilde{g}$), from which we construct a single band using the following parametrization [7]:

$$\delta C_9^{\text{LD}}(q^2) = \frac{a + bq^2(c - q^2)}{q^2(c - q^2)} \tag{5.1}$$

with $a \in [2,7]\,\text{GeV}^4$, $b \in [0.1, 0.2]$ and $c \in [9.3, 9.9]\,\text{GeV}^2$. The resulting band contains all three $\tilde{g}$ functions (and their errors) in the range $1 < q^2 < 9\,\text{GeV}^2$. We add this contribution to each amplitude $\mathcal{A}_i^{L,R}$ by substituting:

$$\mathcal{C}_9 \to \mathcal{C}_9 + s_i \delta C_9^{\text{LD}}(q^2) \ . \tag{5.2}$$

The parameters s_i are varied independently in the range $[-1, 1]$ so that: (i) the contributions to different amplitudes are not artificially correlated, (ii) the possibility of long-distance contribution with opposite signs in the different amplitudes is considered. We emphasize that this method might be overestimating the effect due to (ii) (only one sign corresponds to the computation in ref. [25], the other is only considered here to remain conservative and is not supported by the results of this reference). We also note that the perturbative charm-loop contributions are already included in our predictions up to NLO, while the effects discussed here are the soft-gluon contributions and the non-perturbative extrapolation to $q^2 > 4\,\text{GeV}^2$.

All binned observables are then computed, fixing all parameters to their central values, except for a, b, c and $s_{\perp,\parallel,0}$, which are varied within the given ranges. We perform a random scan over these parameters and obtain maximum and minimum values for each observable. Comparing these values to the results with $s_i = 0$ (which correspond to the central values of our predictions in table 3) we obtain the positive and negative error bars collected in table 4. This procedure will be called approach A in the following. Table 4 summarizes our estimates of these effects. We also show our results in figure 4 where the long-distance $c\bar{c}$ correction is displayed as a separate band. These plots constitute our predictions including charm-loop effects.

In order to be conservative in estimating these error we have also followed another approach B, where we evaluate all relevant observables and check on the difference between

Observable	[0.1,2]	[2,4.3]	[4.3,8.68]	[1,6]	[1,2]	[4.3,6]	[6,8]
$\langle P_1 \rangle$	+0.067 −0.091	+0.041 −0.051	+0.088 −0.061	+0.026 −0.120	+0.089 −0.028	+0.041 −0.028	+0.087 −0.061
$\langle P_2 \rangle$	+0.004 −0.003	+0.052 −0.065	+0.057 −0.048	+0.052 −0.060	+0.011 −0.011	+0.064 −0.063	+0.051 −0.042
$\langle P_4' \rangle$	+0.237 −0.185	+0.095 −0.092	+0.057 −0.089	+0.091 −0.087	+0.118 −0.108	+0.064 −0.076	+0.055 −0.085
$\langle P_5' \rangle$	+0.093 −0.133	+0.098 −0.114	+0.062 −0.082	+0.088 −0.102	+0.090 −0.125	+0.066 −0.079	+0.058 −0.078
$\langle P_3 \rangle$	+0.004 −0.003	+0.009 −0.006	+0.008 −0.006	+0.007 −0.005	+0.007 −0.005	+0.006 −0.004	+0.006 −0.005
$\langle P_6' \rangle$	+0.010 −0.011	+0.005 −0.005	+0.005 −0.005	+0.005 −0.004	+0.008 −0.011	+0.003 −0.003	+0.004 −0.004
$\langle P_8' \rangle$	+0.016 −0.018	+0.005 −0.005	+0.003 −0.004	+0.005 −0.005	+0.009 −0.009	+0.002 −0.003	+0.003 −0.003
$\langle A_{\rm FB} \rangle$	+0.017 −0.010	+0.021 −0.020	+0.051 −0.041	+0.023 −0.021	+0.022 −0.020	+0.034 −0.030	+0.050 −0.042
$\langle F_L \rangle$	+0.062 −0.044	+0.018 −0.019	+0.037 −0.045	+0.021 −0.021	+0.039 −0.039	+0.024 −0.026	+0.037 −0.044
$\langle S_3 \rangle$	+0.015 −0.021	+0.004 −0.005	+0.014 −0.010	+0.003 −0.004	+0.014 −0.018	+0.005 −0.003	+0.015 −0.010
$\langle S_4 \rangle$	+0.049 −0.038	+0.021 −0.019	+0.017 −0.021	+0.022 −0.019	+0.026 −0.022	+0.017 −0.017	+0.016 −0.020
$\langle S_5 \rangle$	+0.032 −0.053	+0.035 −0.039	+0.032 −0.037	+0.034 −0.037	+0.046 −0.060	+0.028 −0.033	+0.031 −0.036
$\langle S_{6s} \rangle$	+0.013 −0.022	+0.027 −0.028	+0.055 −0.068	+0.029 −0.031	+0.026 −0.030	+0.040 −0.046	+0.056 −0.067

Table 4. Estimates for the errors in binned observables arising from long-distance charm-loop effects, as described in the text.
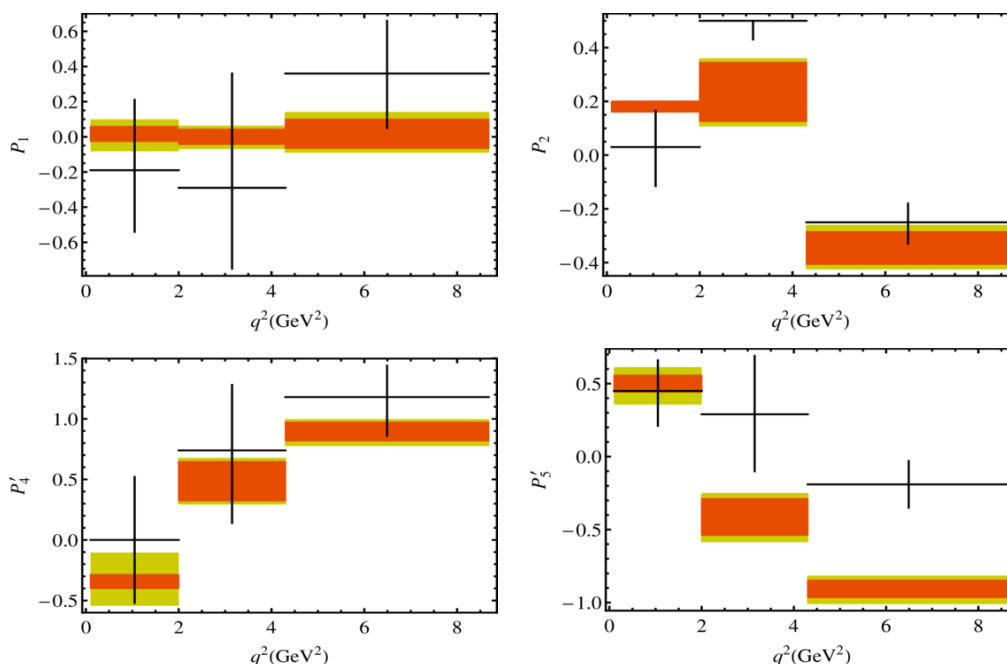

Figure 4. SM predictions for the observables P_1, P_2, P_4', P_5' obtained as described in the text (with form-factor input from [25]). The bands correspond to all uncertainties added in quadrature, not including (dark) and including (light) our estimate of long-distance charm-loop effects. The data points correspond to experimental data from LHCb [1, 2].

the central values obtained including and not including the long-distance contribution described in ref. [25]. In order to do this comparison, we took the charm contribution at the same order and also at the indicated reference mass $m_c(2m_c) = 1.05\,\text{GeV}$ as in ref. [25]. The result of this comparison gives us an estimate of the size of the associated error. Assuming a linear dependence on m_c for the normalisation of the functions $\tilde{g}(1\,\text{GeV}^2)$ as given in table 1 in ref. [25], and translating this into a linear dependence of $\Delta C_9(1\,\text{GeV}^2)$ in eq. (7.14) of the same reference, we have also studied the impact of varying m_c from $1.05\,\text{GeV}$ up to $1.5\,\text{GeV}$. We found that this approach yields an uncertainty substantially smaller than the default approach A outlined above.

Several comments are in order in relation with figure 4 and table 4. First, it appears that the impact of the long-distance contribution remains small up to $8\,\text{GeV}^2$ (even a little bit above $8\,\text{GeV}^2$ the effect is not very significant). Secondly, even if the computation done in ref. [25] implies a definite sign for $\delta C_9^{c\bar{c},\text{LD}}$, following approach A the errors are enlarged to cover the values corresponding to the opposite sign, as we interpret the $\delta C_9^{c\bar{c},\text{LD}}$ extracted from ref. [25] as the expected size of long-distance charm-loop effects rather than taking it at face value. As a third remark, we find that for some observables the slope is more important for the induced uncertainties than the proximity to the resonance region. In other words, an observable with a steep slope like P_5' has a larger error in the intermediate region (from 2 to $6\,\text{GeV}^2$), due to the significant uncertainty on its slope in this region, than in the plateau (from 6 to $8\,\text{GeV}^2$) where the uncertainty is limited. In the case of P_5' in the [6-8] bin, the contribution computed in ref. [25] would tend to enhance the anomaly: however, there is not much space left below the SM prediction without long-distance charm contributions, so that the impact of the latter is small. A similar situation occurs in P_4' but not for P_2.

Other approaches to estimate the uncertainties due to $c\bar{c}$ long-distance contributions could have been followed, but in our opinion, they could yield misleading estimates. First, the original calculation done in ref. [25] re-expresses these long-distance effects, entering in all observables via C_9^{eff} as done here. Other approaches (e.g. ref. [41]) choose to transfer the long-distance effect to C_7. Even though this can always be done in principle, one should be careful to distinguish an estimate of the impact of $c\bar{c}$-loop contributions on C_7 from that on actual observables, as the latter have generally different (and bin-dependent) sensitivities to C_7. Including a specific estimate for charm-loop corrections in C_7 might thus overestimate the uncertainties induced in observables in some energy ranges and underestimate in others.

A second comment concerns the symmetrisation of errors. In the above procedure, we have split ΔC_9 into the contributions from short and long distances in the $c\bar{c}$ contributions as given ref. [25]. Our errors are obtained varying the sign of the long-distance contribution only (the short-distance part being known from perturbation theory). We would have obtained artificially enhanced uncertainties, if we had varied the sign of the whole ΔC_9 contribution, which would have corresponded to a "wrong" sign for the perturbative contribution.

5.3 Comparison with direct form factor approach

As already mentioned, there exist in general two options how to treat the form factors in calculations of $B \to K^* \mu^+ \mu^-$ observables. Our method, to which we will refer here as method I, uses soft form factors complemented with symmetry-breaking $\mathcal{O}(\alpha_s)$-corrections and factorisable power corrections. Alternatively (method II) one can directly use the full QCD form factors, obtained in some particular non-perturbative approach like LCSR which already contain factorisable $\mathcal{O}(\alpha_s)$- and power corrections (see ref. [6]). In both cases one should add also corrections from non-factorisable $\mathcal{O}(\alpha_s)$- and power corrections, including non-perturbative charm-loop effects.

The main difference between the two approaches consists in the fact that method I automatically implements the dominant correlations among form factors via the large-recoil symmetry relations, while method II includes correlations only to the extent they are implemented in the chosen form factor input. This leads to the following consequences:

- Method I can be applied to any given determination of the form factors, without the need of knowing specific details about the computation. Obviously, if correlations are available, they could be included in the extraction of the soft form factors. Method II requires a detailed access of the different steps of the computation chosen, and it cannot be applied unless correlations have been given (or recomputed) as we have illustrated in figure 1. This strongly limits the scope of method II.

- While method II relies on the full set of seven hadronic form factors, method I needs as input only a subset of two form factors forming a soft basis. Method I is thus less sensitive to the form factor input.

- In method I, correlations are explicitly manifest in the splitting between soft form factors and symmetry-breaking corrections. Effects of these correlations can therefore be studied analytically, for example through an explicit cancellation of soft form factors in optimised observables. If correlations are included in method II, they cannot be read off from the analytic expressions because they only work numerically, once a correlated variation of the form factor uncertainties is performed.

- Switching off symmetry-breaking corrections in method I, one can easily reproduce the exact large-recoil symmetry limit. Comparison with the full result gives a quantitative estimate of the validity of large-recoil symmetries and of the size of symmetry-breaking effects. This information is not accessible with method II.

Method II has been applied in refs. [6, 8] for form factor input from ref. [44] using additional (non-public) information on correlations among the form factor uncertainties. This control of correlations is certainly an advantage of the results in refs. [6, 8] compared to our predictions which rely on (correlation-improved) dimensional arguments. Note, however, that origin and extent of the form factor correlations used in refs. [6, 8] are not completely transparent due to the non-public character of the corresponding details of the LCSR calculation. Our results have been given not only for the set of form factors from

ref. [44], but in addition also for input from ref. [25]. Furthermore we provide all details of the analysis that are needed in order to reproduce our results.

6   Conclusions

The rare $B \to K^* \mu^+ \mu^-$ decay has been under recent scrutiny after the LHCb experiment reported deviations with respect to the Standard Model in several observables at large K^* recoil. Following an analysis based on QCD factorisation, these observables $P_i^{(\prime)}$ have been designed to be less sensitive to hadronic uncertainties than the angular coefficients of the differential decay rate. The central issue consists in separating soft contributions $\mathcal{O}(\Lambda)$ from hard contributions $\mathcal{O}(m_b)$ in the expressions of the $B \to K^*$ hadronic form factors and subsequently the helicity amplitudes involved in $B \to K^* \mu^+ \mu^-$ decay, leading to a cancellation of the soft form factors in suitable ratios of angular observables. This cancellation is however only valid at the leading order in QCD factorisation, and the sensitivity to hadronic form factors re-enters through subleading corrections, either hard (computable as a series in α_s) or soft (estimated on dimensional grounds as Λ/m_b).

It was recently claimed that the latter corrections, also known as power corrections, could yield much larger uncertainties than expected for the observables measured at LHCb. This would naturally decrease the sensitivity of these observables to New Physics and reduce the significance of the observed deviations. We have reassessed this claim by adopting and improving the analysis strategy described in ref. [41] to extract the size of the factorisable power corrections, related to the re-expression of the QCD form factors in terms of soft form factors. We consider sets of QCD form factors obtained from light-cone sum rules, identify two soft form factors and compute the central values of factorisable power corrections by taking the difference between QCD form factors and their representation as the sum of soft form factors and perturbative corrections. In order to estimate the uncertainties from factorisable power corrections, we start from a conservative estimate of their overall size based on dimensional arguments. We improve this estimate by systematically taking into account all correlations among the form factors which arise from kinematic identities and from the definition of the renormalisation scheme for the soft form factors. After the QCD form factors are split in their various constituents (soft form factors, perturbative corrections and power corrections), we have shown how to compute observables making the maximal use of the information on the non-zero central values, the uncertainties and the correlations of the power corrections.

It has been demonstrated that in the analysis of factorisable power corrections, the choice of a renormalisation scheme to define the soft form factors out of the QCD form factors has an important impact on the results. Choosing an inappropriate renormalisation scheme, generating large, weakly correlated power corrections for the most relevant form factors for the observables of interest, might lead the factorisable power corrections to induce abnormally large errors for the $B \to K^* \mu^+ \mu^-$ angular observables. We have shown that another (well-documented) scheme yields significantly smaller power corrections than the one chosen in ref. [41] for two different sets of QCD form factors, corresponding to the most recent determinations of QCD form factors based on light-cone sum rules. We have

computed angular observables within this renormalisation scheme, keeping track of the correlations between the various parameters describing the factorisable power corrections. The results for angular observables are collected in table 3 (with a decomposition into the various sources of uncertainties) and illustrated in figure 3 (where results for two different schemes are presented, including non-factorisable corrections). We have also discussed the (small) impact of long-distance contributions from charm loops based on estimates available in the literature, as seen in table 4 and figure 4.

In the process of writing this paper, other issues have been raised concerning the role played by long-distance $c\bar{c}$ loops both for $B \to K \mu^+ \mu^-$ and $B \to K^* \mu\mu$, which are discussed in the appendix of this paper. Both discussions (on the size of power corrections and on the impact of long-distance charmonium dynamics) are useful to reduce the uncertainties attached to the predictions for $B \to K^* \mu^+ \mu^-$ angular observables. A thorough check of the uncertainties attached to these observables is essential to assess the anomaly currently observed in LHCb data, and ultimately confirm its connection with New Physics.

Acknowledgments

A Can charm loops always mimic New Physics?

In a recent article [28], it has been claimed that the observed anomaly in P_5' could be solved thanks to a 350% correction with respect to the factorisation approximation coming from charm-resonance effects.[13] We will not discuss here all the implicit and model-dependent assumptions involved in this approach and necessary to relate $e^+ e^-$ data with the dynamics of charmonia in $B \to K \mu^+ \mu^-$, if the resonance model chosen (with a sum of Breit-Wigner charmonia) can be extrapolated far from the resonance peaks, whether two constant "fudge factors" are enough to capture all the departures of $B \to K \mu^+ \mu^-$ data from this specific resonance model in both low- and large-K recoil regimes, or if the same fudge factors hold unchanged for $B \to K \mu^+ \mu^-$ and $B \to K^* \mu^+ \mu^-$. Instead we will take the solution proposed in ref. [28], which implies a very specific q^2-dependent form for long-distance $c\bar{c}$ contributions and propose three different tests that can be implemented to assess the validity of this proposal.

A fit to all $b \to s\ell\ell$ observables including this model of contribution for long-distance $c\bar{c}$ loops could shed some light on the global coherence of such a proposal, even though a likely outcome of this fit would be a slight improvement compared to the standard modelisation,

---

[13]For simplicity, we call "charm-resonance effects" a contribution from charm loops following ref. [28], irrespectively of its origin (long-distance QCD and/or new $\bar{b}sc\bar{c}$ structures). The term "New Physics" will be used exclusively to refer to a new high-scale contribution to one of the Wilson coefficients $C_i^{(\prime)}$ $i = 7, 9, 10$.

as it would include two new free parameters. In this situation, more specific observables could provide a more clear-cut test of this model for charm-loop contributions. We start defining the semileptonic coefficients as in ref. [28]

$$C_9^{\mathrm{eff}} = C_9 + a_{fac}\eta_c h_c(q^2) + h_{\mathrm{rest}}(q^2), \qquad C_9'^{\mathrm{eff}} = C_9' + a_{fac}\eta_c' h_c(q^2), \qquad (A.1)$$

where $a_{fac} \sim 0.6$ stems from factorisation, η_c and η_c' are pre-factor parameters found to be large and negative from the analysis of low-recoil $B \to K\mu^+\mu^-$ differential branching ratio (whereas the standard expectations would be $\eta_c = 1, \eta_c' = 0$). The function $h_c(q^2)$ describes long- and short-distance from charm loops, through a dispersive relation applied to a Breit-Wigner model for the observed $c\bar{c}$ resonances in $\sigma(e^+e^- \to \mathrm{hadrons})$. $h_{\mathrm{rest}}(q^2)$ stands for the sub-leading contributions from other flavours which are very tiny and will be neglected for the rest of the discussion.

It was argued in ref. [28] that the result of fitting the data at low recoil for $\mathcal{B}(B^+ \to K^+\mu^+\mu^-)$, sensitive to the sum $C_9^+ = C_9^{\mathrm{eff}} + C_9'^{\mathrm{eff}}$, imposes

$$\eta_c + \eta_c' \sim -2.5 \qquad (A.2)$$

It is important to remark at this point that ref. [28] assumes implicitly that the Standard Model holds in order to obtain eq. (A.2) by combining e^+e^- data with $\mathcal{B}(B^+ \to K^+\mu^+\mu^-)$ data. Indeed, if New Physics affected $B \to K\mu^+\mu^-$ data, the sum eq. (A.2) could be reduced substantially, so that charm-resonance effect could not accommodate the P_5' anomaly contrary to what is stated in ref. [28].

Our approach here is to explore patterns in designed observables that cannot be explained in the Standard Model by the modification of the prefactors η_c and η_c' to the charm-loop contribution entering C_9^{eff} and $C_9'^{\mathrm{eff}}$ as proposed in ref. [28]. Such patterns would thus require New Physics even if the charm loop model of ref. [28] is valid. In the following, we will mostly work under the hypothesis of no New Physics

$$C_{7,9,10}^{NP} = 0, \qquad C_{7,9,10}' = 0. \qquad (A.3)$$

Within this framework $C_9'^{\mathrm{eff}}$ would contain only $a_{fac}\eta_c' h_c(q^2)$ but not New Physics. However, in some cases we will relax this hypothesis and allow for New Physics to illustrate how certain conditions change.

The authors of ref. [28] find in agreement with ref. [7] that in order to explain the $B \to K^*\mu^+\mu^-$ anomaly, a scenario is favoured where the (effective) Wilson coefficients C_9^{eff} and $C_9'^{\mathrm{eff}}$ receive new contributions with $\Delta C_9^{\mathrm{eff}} \simeq \Delta C_9'^{\mathrm{eff}}$. They claim that these new contributions could be generated from resonant charm loops rather than from high-scale new physics. In this appendix we discuss three tests on the forthcoming data which could disentangle the two proposals. The first test will consist in identifying an observable for which the charm-loop contribution eqs. (A.1)–(A.2) alone cannot mimic the contribution from a New Physics source. The second test is based on observing the presence of these charm contributions in the related $b \to d$ transition decay $B \to \pi\mu^+\mu^-$. Finally, the third more qualitative test aims at disentangling the effect of two large negative parameters η_c, η_c' from a true New Physics contribution to C_9 and C_9'.

A.1 Test 1: P_1 strikes back

Our first test will focus on $B \to K^* \mu^+ \mu^-$ angular observables for which specific values cannot be accommodated by the charm-loop model eqs. (A.1)–(A.2) but are allowed in New Physics models. If eq. (A.2) holds, the largest impact of this charm-loop model should be expected in observables sensitive to C_9^+. In the context of the $B \to K^* \mu^+ \mu^-$ decay the inspection of the transversity amplitudes (see [5]) suggests that an observable proportional to $A_\perp^{L,R}$ will do the job, such as

$$Q_{[6 \leq q^2 \leq 8]}(q^2) = 1 + P_1(q^2) = \frac{2|A_\perp|^2}{|A_\perp|^2 + |A_\parallel|^2} \tag{A.4}$$

where it is understood that $|A_i|^2 = |A_i^L|^2 + |A_i^R|^2$ is the sum of the corresponding left and right transversity amplitudes and the subscript indicates the relevant range for q^2. From this observable Q one immediately obtains two more observables

$$R = Q \times F_T = F_T + 2S_3, \qquad S = R \times d\Gamma/dq^2.$$

As a probe of the Wilson coefficients, S plays in $B \to K^* \mu^+ \mu^-$ a similar role to $\mathcal{B}(B \to K \mu^+ \mu^-)$. Both are only a function of $C_9^+ = C_9^{\text{eff}} + C_9'^{\text{eff}}$, contrary to $\mathcal{B}(B \to K^* \mu^+ \mu^-)$ which is a function of C_9^+ and $C_9^- = C_9^{\text{eff}} - C_9'^{\text{eff}}$.

LHCb [2] found for the wide third bin

$$Q_{[4.3 \leq q^2 \leq 8.68]} \sim 1.36 \pm 0.30 \tag{A.5}$$

There is also a previous measurement by CDF [46, 47] but with a very large uncertainty.

One can understand the discriminating power of this observable with the following argument.[14] In the SM within the large-recoil range but for q^2 not small (between 6 to $8\,\text{GeV}^2$), the electromagnetic piece of the amplitude proportional to C_7 is subleading and the semileptonic contributions linked to $C_{9,10}$ dominate. At leading order one can approximate this observable in this region as

$$Q_{[6 \leq q^2 \leq 8]}(q^2) \sim \frac{|C_9^+|^2 + |C_{10}|^2}{|C_9^+|^2/2 + |C_9^-|^2/2 + |C_{10}|^2} \tag{A.6}$$

In the standard case $\eta_c = 1, \eta_c' = 0$ which implies $C_9^+ = C_9^-$ and $Q_{[6 \leq q^2 \leq 8]} \sim 1$ (in agreement with our SM prediction of $P_1^{[6,8]} = 0.015^{+0.088}_{-0.080}$).

Under the hypothesis that future data will significantly increase the significance of the deviation from one of eq. (A.5) we will explore the implication of the condition $Q_{[6 \leq q^2 \leq 8]} > 1$, which translates using eq. (A.6) into the constraint

$$\text{Re} C_9^{\text{eff}} C_9'^{\text{eff}*} > 0 \quad \Rightarrow \quad (C_9 + a_{fac} \eta_c \text{Re} h_c)(a_{fac} \eta_c' \text{Re} h_c) > 0 \tag{A.7}$$

where h_c is real in this region according to ref. [28]. This equation requires the same sign for C_9^{eff} and $C_9'^{\text{eff}}$, which implies two solutions for η_c, η_c':

---

[14]We will not consider the impact of power corrections here. In any case, we have seen that at most they tend to shift up P_1 approximately by $+0.11$ in this bin, which can be expected to be the maximum value above zero reached by this bin within the SM. A scan over η_c and η_c' satisfying eq. (A.2) confirms this expectation.

I. $\eta_c' < 0$ (both coefficients negative): then using eq. (A.2) and eq. (A.7) one finds

$$-2.5 < \eta_c < \text{Max}[-C_9/(a_{fac}\text{Re}h_c)]_{[6\leq q^2\leq 8]} = -2.6$$

This condition is obviously impossible to fulfil. The right-hand side term reaches its maximum at $q^2 = 8\,\text{GeV}^2$ defining the most favourable situation, still impossible to satisfy. This is not surprising because the sign of C_9^{eff} can be changed only for very large negative η_c. Notice that even if at first sight a NP contribution of the type $C_9^{NP} < 0$ could extend the allowed range and allow this solution, one should first reassess the determination of $\eta_c + \eta_c'$ which was performed in the SM, and second, check that this value of η_c allows for a zero in A_{FB} (see Test 3 below).

II. $\eta_c' > 0$ (both coefficients positive): then using the same equations one gets

$$-2.5 > \eta_c > \text{Min}[-C_9/(a_{fac}\text{Re}h_c)]_{[6\leq q^2\leq 8]} = -4.3$$

This range of values for η_c is also excluded because for these values of η_c, P_2 (or A_{FB}) has no zero (see Test 3).

The power of this test can be illustrated by the cases considered in ref. [28]. One of the illustrative examples ($\eta_c = 0, \eta_c' = -2.5$) in ref. [28] yields $Q \sim 0.5$ in the bin [4.3,8.68][15] which is disfavoured by LHCb measurements, and another one ($\eta_c = -2.5, \eta_c' = 0$) is also disfavoured due to the lack of zero in A_{FB} (or P_2) (see Test 3 and figure 12 in ref. [28]).

In summary, if an accurate measurement of the last bin of P_1 (bin [6,8]) shows a clear preference for $Q_{[6,8]} > 1$, it cannot be accommodated by the solution $\eta_c + \eta_c' \sim -2.5$ *with no New Physics contributions.*

A value of $Q_{[6,8]}$ exceeding its SM prediction $Q \sim 1.11$ can be attained in the presence of certain NP, for example in the presence right-handed currents. The subleading terms in $Q_{[6,8]}$ can become important when NP is present: for instance, if $C_7' \sim 0.06$, $C_{10}' \sim -1$ and $C_9^{NP} \sim -1$ (allowed at 2σ according to ref. [7]) a large deviation of order $Q \sim 1.4$ is generated while keeping $\eta_c = 1$ and $\eta_c' = 0$. Notice that if NP is also switched on, a solution with $\eta_c \neq 1$ and $\eta_c' \neq 0$ is allowed. This test (if $Q > 1$) provides an explicit example where eqs. (A.1)–(A.2) alone would fail in giving an explanation, unless New Physics is allowed. In this sense this first test should be understood more as a test on the presence of New Physics generating $Q > 1$ that cannot be polluted by charm loop than a test of eqs. (A.1)–(A.2) themselves. In the case where $Q \sim 1$ the test loses its discriminating power.

Finally, let us recall that P_1 is constrained by P_4' by $P_1 \leq 1 - P_4'^2$ [48]. A measurement of the [6,8] bin of P_4' constrains $Q_{[6\leq q^2\leq 8]} \leq 2 - P_{4\,[6\leq q^2\leq 8]}'^2$ (up to small corrections due to binning).

---

[15]P_1 and consequently Q can be inferred from the values of P_2 and $P_{4,5}'$ in [48] (see also eq. (A.12)) or determined by direct computation.

A.2 Test 2: $B^+ \to \pi^+ \mu^+ \mu^-$

This test relies on the similarities and differences between $B^+ \to K^+ \mu^+ \mu^-$ and $B^+ \to \pi^+ \mu^+ \mu^-$ decays. Since $B^+ \to K^+ \mu^+ \mu^-$ is a $b \to s$ transition while $B^+ \to \pi^+ \mu^+ \mu^-$ comes from $b \to d$, New Physics will affect them differently: in certain models one could expect to see a deviation in the $b \to s$ transition and no deviation in the corresponding $b \to d$ decay. Under these circumstances, the large impact of the charm loop model eqs. (A.1)–(A.2) should affect both decays and could be tested directly. One would expect to see the same pattern in $\mathcal{B}(B^+ \to K^+ \mu^+ \mu^-)$ and in $\mathcal{B}(B^+ \to \pi^+ \mu^+ \mu^-)$ in the low-q^2 region $(1 \le q^2 \le 8\,\text{GeV}^2)$, namely values below the SM prediction due to the large destructive charm-loop interference.

One should however take care of the different CKM structure involved in the two decays. The charm loop has the CKM coefficient $V_{cb}V_{cD}^* = -V_{tb}V_{tD}^*(1 + V_{ub}V_{uD}^*/V_{tb}V_{tD}^*)$ (with $D = d, s$). Whereas the second term is doubly Cabibbo-suppressed for $D = s$, it remains Cabibbo-allowed for $D = d$ and should be included in the discussion, as shown in eq. (16) of ref. [49]. When moving from $b \to s$ to $b \to d$ the coefficient in front of the charm loop inside C_9^{eff} becomes

$$h(m_c, q^2) \to \left(1 - \frac{R_b}{R_t}e^{i\alpha}\right) h(m_c, q^2) \tag{A.8}$$

Taking $R_b/R_t \sim 0.4$ and $\alpha \sim 90°$ the real part of the coefficient remains positive and dominates. Thus, following ref. [28] and substituting h_c by $\eta_c h_c$ (with η_c a large negative parameter), one would expect to see a suppression of $\mathcal{B}(B^+ \to \pi^+ \mu^+ \mu^-)$ with respect to the SM prediction with $\eta_c = 1$, $\eta_c' = 0$. Indeed, as can be seen from ref. [49], this branching ratio involves $|C_9^+|^2$, and an illustrative back-of-the-envelope computation indicates that for $q^2 = 8\,\text{GeV}^2$, one has $C_9^+ \sim 0.2 + i1.6$ and $|C_9^+|^2 \sim 2.5$ for $\eta_c + \eta_c' = -2.5$, whereas $C_9^+ \sim 5.6 - i0.6$ and $|C_9^+|^2 \sim 32.1$ for $\eta_c + \eta_c' = 1$, confirming the expected suppression of $\mathcal{B}(B^+ \to \pi^+ \mu^+ \mu^-)$ with respect to the SM prediction with $\eta_c = 1$, $\eta_c' = 0$. Also one should take into account when comparing those modes the possible impact of annihilation contributions (see, for instance, [50] for $B \to K$ case).

In summary, a measurement of $\mathcal{B}(B^+ \to \pi^+ \mu^+ \mu^-)$ in the low-q^2 region $(1 \le q^2 \le 8\,\text{GeV}^2)$ above the SM or in perfect agreement with SM would disfavour the charm-loop destructive effect eqs. (A.1)–(A.2). On the contrary if data in this region is below the SM prediction as in $\mathcal{B}(B^+ \to K^+ \mu^+ \mu^-)$, one cannot disentangle between a charm loop effect or a New Physics effect affecting also the $b \to d$ transition. The present situation is that there is a first measurement done by LHCb [51] in the entire range of q^2

$$\mathcal{B}(B^+ \to \pi^+ \mu^+ \mu^-) = (2.3 \pm 0.6(\text{stat.}) \pm 0.1(\text{syst.})) \times 10^{-8}$$

and two compatible SM theory predictions $\mathcal{B}(B^+ \to \pi^+ \mu^+ \mu^-) = (1.88^{+0.32}_{-0.21}) \times 10^{-8}$ [49] and $\mathcal{B}(B^+ \to \pi^+ \mu^+ \mu^-) = (2.0 \pm 0.2) \times 10^{-8}$ [52]. Even if this comparison would seem to be already now in conflict with the model in ref. [28], we insist that the comparison must be done only in the low-q^2 region, where the discussion is much simpler due to the absence of resonances. According to ref. [49] the SM prediction is, with $\eta_c = 1$, $\eta_c' = 0$,

$$\mathcal{B}(B^+ \to \pi^+ \mu^+ \mu^-)_{[1 \le q^2 \le 8]} = (0.58^{+0.09}_{-0.06}) \times 10^{-8}$$

If LHCb measures this bin with a measurement above or in agreement with this value, the charm-loop model eqs. (A.1)–(A.2) would need to be revised.

A.3 Test 3: zeroes and branching ratio

This third category of tests will be focused on identifying observables able to disentangle the large contributions from the long-distance charm-loop model eqs. (A.1)–(A.2) from a New Physics contribution to the short-distance Wilson coefficients. We will focus first on the zero/zeroes of the observable P_2 and consider later the behaviour of the branching ratio of $B \to K\mu^+\mu^-$ at the upper end of the large-recoil region. We should remark that this last category of tests is extremely challenging experimentally.

An independent constraint on η_c in the SM comes from the existence of a zero in P_2 (or A_{FB}).[16] At leading order, η_c must fulfil the equation

$$-2m_b M_B C_7^{\text{eff}} \frac{1}{s_i} = C_9 + a_{fac}\eta_c \text{Re}h_c(s_i) \tag{A.9}$$

where s_i stands for the zero(es) in q^2. We can impose that there must exist a zero at leading order (at NLO the position of the zero is typically shifted by $\sim 1\,\text{GeV}^2$) between, say, 2 and $6\,\text{GeV}^2$ (a smaller allowed range in q^2 implies a stronger constraint on η_c). Using our inputs and the variation of h_c in this range, we find that

$$\eta_c \gtrsim -2 \tag{A.10}$$

Combining this bound with the solution eq. (A.2) advocated in ref. [28], we see that η_c' cannot vanish. If New Physics is allowed only in C_9 and C_9' (but not in C_{10}'), eq. (A.9) is unchanged but the bound becomes more constraining in the case of a negative New Physics contribution to C_9, reducing substantially the impact of the charm loop on C_9^{eff}:

$$\eta_c \gtrsim -2 - C_9^{NP}/(a_{fac}\text{Re}h_c(s_i)) \tag{A.11}$$

Using appendix B of ref. [5] one can easily generalise this expression to NP affecting other Wilson coefficients.

Eq. (A.9) also shows that for a subset of *negative* values for η_c fulfilling the bound eq. (A.10), a second zero in P_2 would arise at a higher value of q^2 still within the large-recoil region. Notice that there is no second zero if $\eta_c = 1$, with or without New Physics. The observation of a second zero *below* $8\,\text{GeV}^2$ would give a strong hint in favour of the charm-loop model eqs. (A.1)–(A.2). Conversely, not finding this second zero does not disprove directly this model, but it would push η_c' towards large negative values implying a large negative $C_9'^{\text{eff}}$ that has to be tested against other observables. However, checking if such a second zero exists so close to $8\,\text{GeV}^2$ seems very challenging from the experimental point of view.

Further comments are in order concerning how a value of $\eta_c \neq 1$ would affect various observables at the upper end of the large-recoil region. One can also see that P_2 and P_5' should vanish at the J/ψ peak — and the speed at which they tend to zero is related to

---

[16]LHCb [1] found a zero in A_{FB} at $q_0^2 = 4.9 \pm 0.9\,\text{GeV}^2$.

h_c. The reason is that in the numerator of these observables there is a cancellation of the quadratic term in C_9^{eff} (see appendix B in [5]) which implies that the numerator is at most linear in the function $h_c(s)$. This cancellation does not occur in the denominator that contains terms proportional to $h_c(s)^2$. If $\eta_c = 1$ the divergent behaviour of $h_c(s)$ is not visible until $q^2 > 8.5\,\text{GeV}^2$ but for large and negative η_c the effect of the divergence is enhanced and the tendency to zero should be more evident before $8\,\text{GeV}^2$. Let us stress that this vanishing behaviour is different from the second zero of P_2 discussed in the previous paragraph.

As a side remark it is interesting to notice that the zeroes of P_2 are related to the sign of P_5'. One can show easily using the relation [48]

$$P_2 = \frac{1}{2}\left[P_4' P_5' + \sqrt{(-1 + P_1 + P_4'^2)(-1 - P_1 + P_5'^2)} \right] \tag{A.12}$$

that at the point where $P_2 = 0$, eq. (A.12) requires P_5' to be negative (given that $P_4' > 0$ in agreement with data), which implies by continuity that the curve of P_5' is below P_2 in the vicinity of the points where $P_2 = 0$. This should happen independently of the value of η_c and at each zero. Interestingly, this might have implications on the relative positions of P_2 and P_5' in the bins near the zero(es) of P_2.

Finally, an important difference between refs. [28] and [7] comes from the q^2-dependence of the Wilson coefficients. In the charm-loop model eqs. (A.1)–(A.2), C_9^+ decreases with q^2. The same occurs for C_9^{eff} if η_c is negative. In ref. [7] where $\eta_c = 1$ and $\eta_c' = 0$, both C_9^+ and C_9^{eff} increase with q^2. If $\eta_c + \eta_c'$ turns out to be large and negative, this should be seen in observables sensitive to C_9^+: for instance $\mathcal{B}(B \to K \mu^+ \mu^-)$ or S should exhibit a more pronounced suppression from [4.3,6] to [6,8] than expected from a standard calculation using $\eta_c = 1$ (see figure 10 in ref. [53]).

In summary the tests proposed in this section aim at disentangling a New Physics contribution to C_9 from a charm loop effect. They rely on the behaviour induced by the charm-loop model in ref. [28] in angular observables at the upper end of the large-recoil region, where the sensitivity to a large negative η_c parameter (if any) should be more visible. The required accuracy to perform such tests exceeds what can be achieved experimentally for the moment, but presents very interesting challenges for the future.

B   Factorisable α_s corrections

In this appendix we collect the expressions for the factorisable α_s corrections ΔF^{α_s} appearing in the soft form factor representation eq. (2.1). They can be found in ref. [29] where they have been derived for a renormalization scheme defining $\xi_\perp$ and $\xi_\parallel$ in terms of V and A_0. Translating their results to our preferred scheme with $(\xi_\perp^{(1)}, \xi_\perp^{(1)})$ defined from

(V, A_1, A_2) we obtain

$$\Delta V^{(1)\alpha_s} = 0,$$
$$\Delta A_1^{(1)\alpha_s} = \Delta A_2^{(1)\alpha_s} = \mathcal{O}(\alpha_s^2),$$
$$\Delta A_0^{(1)\alpha_s} = \frac{E(q^2)}{m_{K^*}} \xi_\parallel^{(1)}(q^2) \left(\frac{1}{\Delta} - 1 \right),$$
$$\Delta T_1^{(1)\alpha_s} = C_F \alpha_s(\mu_b) \xi_\perp^{(1)}(q^2) \left[\log \frac{m_b^2}{\mu_b^2} - L \right] + C_F \alpha_s(\mu_b)\, \delta T_1, \qquad \text{(B.1)}$$
$$\Delta T_2^{(1)\alpha_s} = C_F \alpha_s(\mu_b) \frac{2E(q^2)}{m_B} \xi_\perp^{(1)}(q^2) \left[\log \frac{m_b^2}{\mu_b^2} - L \right] + C_F \alpha_s(\mu_h)\, \delta T_2,$$
$$\Delta T_3^{(1)\alpha_s} = C_F \alpha_s(\mu_b) \left(\xi_\perp^{(1)}(q^2) \left[\log \frac{m_b^2}{\mu_b^2} - L \right] - \xi_\parallel^{(1)}(q^2) \left[\log \frac{m_b^2}{\mu_b^2} + 2L \right] \right) + C_F \alpha_s(\mu_h)\, \delta T_3,$$

where $L = -(2E/(m_B - 2E)) \log(2E/m_B)$, μ_b and μ_h are typical scales for hard processes and Δ is defined in eq. (66) of [30]. The spectator scattering terms are given by

$$\delta T_1 = \frac{m_B}{4E} \Delta F_\perp, \qquad \delta T_2 = \frac{1}{2} \Delta F_\perp, \qquad \delta T_3 = \delta T_1 + 2 \frac{m_{K^*}}{m_B} \left(\frac{m_B}{2E} \right)^2 \Delta F_\parallel, \qquad \text{(B.2)}$$

with $\Delta F_{\perp,\parallel}$ defined in eq. (59) of [29]. In the scheme with $(\xi_\perp^{(2)}, \xi_\perp^{(2)})$ defined from (T_1, A_0) we get

$$\Delta V^{(2)\alpha_s} = -\frac{m_B + m_{K^*}}{m_B} \left\{ C_F \alpha_s(\mu_b) \xi_\perp^{(2)} \left[\log \frac{m_b^2}{\mu_b^2} - L \right] + C_F \alpha_s(\mu_h)\, \delta T_1 \right\},$$
$$\Delta A_1^{(2)\alpha_s} = -\frac{2E}{m_B + m_{K^*}} \left\{ C_F \alpha_s(\mu_b) \xi_\perp^{(2)} \left[\log \frac{m_b^2}{\mu_b^2} - L \right] + C_F \alpha_s(\mu_h) \delta T_1 \right\},$$
$$\Delta A_2^{(2)\alpha_s} = -\frac{m_B}{m_B - m_{K^*}} \left\{ C_F \alpha_s(\mu_b) \xi_\perp^{(2)} \left[\log \frac{m_b^2}{\mu_b^2} - L \right] - (\Delta - 1)\xi_\parallel^{(2)} + C_F \alpha_s(\mu_h)\, \delta T_1 \right\},$$
$$\Delta A_0^{(2)\alpha_s} = \Delta T_1^{(2)\alpha_s} = 0,$$
$$\Delta T_2^{(2)\alpha_s} = C_F \alpha_s(\mu_h) \left(\delta T_2 - \frac{2E}{m_B} \delta T_1 \right),$$
$$\Delta T_3^{(2)\alpha_s} = \xi_\parallel^{(2)} \left\{ \Delta \left(1 + C_F \alpha_s(\mu_b) \left[\log \frac{m_b^2}{\mu_b^2} + 2L \right] \right) - 1 \right\} + C_F \alpha_s(\mu_h)(\delta T_3 - \delta T_1). \quad \text{(B.3)}$$

C SM predictions for other $B \to K^* \mu^+ \mu^-$ observables

Here we collect the SM predictions for other observables not given in section 5, as computed following the approach explored in this paper. Again, we collect for references the results in our preferred scheme 1, corresponding to defining the soft form factors from V, A_1, A_2.

Observable	KMPW - scheme 1	BZ - scheme 1
$\langle P_3\rangle_{[0.1,2]}$	$-0.001^{+0.000+0.000+0.000+0.017}_{-0.000-0.000-0.000-0.018}$	$-0.002^{+0.000+0.000+0.000+0.017}_{-0.000-0.000-0.001-0.019}$
$\langle P_3\rangle_{[2,4.3]}$	$0.002^{+0.001+0.004+0.003+0.005}_{-0.001-0.002-0.003-0.005}$	$-0.003^{+0.000+0.000+0.003+0.003}_{-0.001-0.000-0.003-0.003}$
$\langle P_3\rangle_{[4.3,8.68]}$	$0.003^{+0.000+0.005+0.003+0.003}_{-0.003-0.002-0.002-0.002}$	$-0.003^{+0.001+0.000+0.002+0.003}_{-0.000-0.000-0.002-0.002}$
$\langle P_3\rangle_{[1,6]}$	$0.002^{+0.001+0.003+0.003+0.005}_{-0.000-0.002-0.002-0.006}$	$-0.003^{+0.000+0.000+0.002+0.004}_{-0.001-0.000-0.002-0.004}$
$\langle P_3\rangle_{[1,2]}$	$-0.001^{+0.000+0.001+0.002+0.016}_{-0.000-0.000-0.002-0.017}$	$-0.003^{+0.000+0.000+0.002+0.016}_{-0.001-0.000-0.002-0.018}$
$\langle P_3\rangle_{[4.3,6]}$	$0.003^{+0.002+0.004+0.003+0.001}_{-0.001-0.002-0.002-0.001}$	$-0.002^{+0.000+0.000+0.002+0.002}_{-0.001-0.000-0.002-0.001}$
$\langle P_3\rangle_{[6,8]}$	$0.002^{+0.002+0.004+0.002+0.002}_{-0.004-0.002-0.002-0.002}$	$-0.002^{+0.002+0.000+0.002+0.003}_{-0.001-0.000-0.001-0.002}$
$\langle P'_6\rangle_{[0.1,2]}$	$-0.071^{+0.022+0.012+0.004+0.014}_{-0.030-0.013-0.006-0.015}$	$-0.074^{+0.024+0.001+0.005+0.015}_{-0.031-0.001-0.006-0.016}$
$\langle P'_6\rangle_{[2,4.3]}$	$-0.084^{+0.027+0.018+0.002+0.009}_{-0.036-0.020-0.002-0.008}$	$-0.084^{+0.028+0.001+0.002+0.009}_{-0.035-0.001-0.002-0.008}$
$\langle P'_6\rangle_{[4.3,8.68]}$	$-0.067^{+0.039+0.020+0.003+0.011}_{-0.020-0.022-0.003-0.013}$	$-0.063^{+0.037+0.001+0.003+0.012}_{-0.016-0.001-0.003-0.014}$
$\langle P'_6\rangle_{[1,6]}$	$-0.076^{+0.025+0.017+0.002+0.008}_{-0.036-0.019-0.002-0.007}$	$-0.075^{+0.026+0.001+0.002+0.008}_{-0.033-0.001-0.002-0.007}$
$\langle P'_6\rangle_{[1,2]}$	$-0.089^{+0.026+0.015+0.006+0.015}_{-0.036-0.016-0.007-0.016}$	$-0.093^{+0.029+0.001+0.007+0.016}_{-0.037-0.001-0.007-0.017}$
$\langle P'_6\rangle_{[4.3,6]}$	$-0.061^{+0.022+0.016+0.003+0.007}_{-0.039-0.020-0.003-0.007}$	$-0.058^{+0.022+0.001+0.003+0.007}_{-0.036-0.001-0.003-0.008}$
$\langle P'_6\rangle_{[6,8]}$	$-0.059^{+0.055+0.017+0.003+0.012}_{-0.045-0.021-0.003-0.014}$	$-0.056^{+0.052+0.001+0.003+0.013}_{-0.045-0.001-0.003-0.015}$
$\langle P'_8\rangle_{[0.1,2]}$	$0.032^{+0.027+0.015+0.007+0.014}_{-0.017-0.014-0.006-0.015}$	$0.034^{+0.027+0.001+0.007+0.014}_{-0.017-0.001-0.006-0.016}$
$\langle P'_8\rangle_{[2,4.3]}$	$0.058^{+0.036+0.019+0.005+0.010}_{-0.023-0.015-0.005-0.012}$	$0.057^{+0.034+0.001+0.004+0.010}_{-0.023-0.001-0.004-0.012}$
$\langle P'_8\rangle_{[4.3,8.68]}$	$0.053^{+0.018+0.020+0.001+0.006}_{-0.041-0.016-0.001-0.008}$	$0.049^{+0.015+0.001+0.002+0.006}_{-0.037-0.001-0.002-0.008}$
$\langle P'_8\rangle_{[1,6]}$	$0.051^{+0.035+0.018+0.004+0.009}_{-0.021-0.014-0.004-0.010}$	$0.050^{+0.032+0.001+0.004+0.009}_{-0.021-0.001-0.003-0.010}$
$\langle P'_8\rangle_{[1,2]}$	$0.049^{+0.035+0.017+0.009+0.015}_{-0.022-0.015-0.008-0.018}$	$0.052^{+0.034+0.001+0.009+0.016}_{-0.023-0.001-0.008-0.018}$
$\langle P'_8\rangle_{[4.3,6]}$	$0.046^{+0.037+0.017+0.002+0.006}_{-0.019-0.013-0.002-0.007}$	$0.043^{+0.034+0.001+0.002+0.006}_{-0.018-0.000-0.002-0.007}$
$\langle P'_8\rangle_{[6,8]}$	$0.047^{+0.038+0.019+0.001+0.007}_{-0.059-0.015-0.001-0.008}$	$0.044^{+0.036+0.001+0.001+0.006}_{-0.053-0.001-0.001-0.008}$
$\langle A_{\mathrm{FB}}\rangle_{[0.1,2]}$	$-0.131^{+0.002+0.068+0.005+0.000}_{-0.001-0.058-0.004-0.000}$	$-0.123^{+0.004+0.007+0.007+0.000}_{-0.002-0.006-0.005-0.000}$
$\langle A_{\mathrm{FB}}\rangle_{[2,4.3]}$	$-0.080^{+0.020+0.052+0.032+0.005}_{-0.013-0.085-0.033-0.004}$	$-0.047^{+0.017+0.004+0.029+0.005}_{-0.013-0.003-0.033-0.003}$
$\langle A_{\mathrm{FB}}\rangle_{[4.3,8.68]}$	$0.175^{+0.024+0.173+0.022+0.002}_{-0.014-0.13\ -0.025-0.002}$	$0.204^{+0.020+0.012+0.018+0.002}_{-0.012-0.014-0.024-0.002}$
$\langle A_{\mathrm{FB}}\rangle_{[1,6]}$	$-0.042^{+0.021+0.025+0.030+0.004}_{-0.012-0.027-0.031-0.003}$	$-0.013^{+0.018+0.001+0.027+0.004}_{-0.010-0.000-0.031-0.003}$
$\langle A_{\mathrm{FB}}\rangle_{[1,2]}$	$-0.199^{+0.010+0.128+0.021+0.004}_{-0.006-0.21\ \ -0.019-0.002}$	$-0.174^{+0.012+0.015+0.020+0.004}_{-0.009-0.014-0.018-0.003}$
$\langle A_{\mathrm{FB}}\rangle_{[4.3,6]}$	$0.086^{+0.025+0.121+0.028+0.002}_{-0.011-0.066-0.031-0.002}$	$0.118^{+0.020+0.008+0.024+0.002}_{-0.010-0.009-0.030-0.002}$
$\langle A_{\mathrm{FB}}\rangle_{[6,8]}$	$0.202^{+0.028+0.184+0.021+0.002}_{-0.013-0.148-0.023-0.002}$	$0.231^{+0.023+0.013+0.017+0.003}_{-0.011-0.015-0.022-0.002}$

Table 5. SM predictions for P_3, P'_6, P'_8, A_{FB} in various bins. Same notation as table 3.

Observable	KMPW - scheme 1	BZ - scheme 1
$\langle F_L \rangle_{[0.1,2]}$	$0.345^{+0.028+0.278+0.050+0.010}_{-0.022-0.229-0.045-0.008}$	$0.400^{+0.030+0.029+0.048+0.011}_{-0.026-0.024-0.045-0.009}$
$\langle F_L \rangle_{[2,4.3]}$	$0.763^{+0.011+0.148+0.018+0.003}_{-0.009-0.294-0.021-0.003}$	$0.784^{+0.011+0.018+0.016+0.002}_{-0.010-0.016-0.016-0.002}$
$\langle F_L \rangle_{[4.3,8.68]}$	$0.648^{+0.006+0.244+0.012+0.004}_{-0.003-0.298-0.013-0.004}$	$0.638^{+0.008+0.024+0.014+0.004}_{-0.006-0.021-0.015-0.004}$
$\langle F_L \rangle_{[1,6]}$	$0.717^{+0.010+0.179+0.021+0.004}_{-0.010-0.305-0.022-0.003}$	$0.736^{+0.011+0.021+0.019+0.003}_{-0.011-0.019-0.018-0.003}$
$\langle F_L \rangle_{[1,2]}$	$0.630^{+0.030+0.203+0.048+0.010}_{-0.025-0.32\ -0.049-0.008}$	$0.688^{+0.027+0.023+0.039+0.009}_{-0.026-0.021-0.044-0.007}$
$\langle F_L \rangle_{[4.3,6]}$	$0.710^{+0.005+0.199+0.011+0.002}_{-0.004-0.302-0.013-0.002}$	$0.708^{+0.008+0.022+0.013+0.002}_{-0.007-0.020-0.015-0.002}$
$\langle F_L \rangle_{[6,8]}$	$0.631^{+0.007+0.257+0.013+0.004}_{-0.004-0.297-0.013-0.004}$	$0.617^{+0.009+0.024+0.015+0.004}_{-0.006-0.021-0.016-0.004}$
$\langle S_3 \rangle_{[0.1,2]}$	$0.005^{+0.000+0.004+0.002+0.008}_{-0.000-0.003-0.002-0.010}$	$0.007^{+0.001+0.000+0.002+0.007}_{-0.001-0.000-0.002-0.009}$
$\langle S_3 \rangle_{[2,4.3]}$	$0.000^{+0.000+0.000+0.004+0.001}_{-0.000-0.001-0.004-0.001}$	$-0.003^{+0.000+0.000+0.004+0.000}_{-0.000-0.000-0.005-0.000}$
$\langle S_3 \rangle_{[4.3,8.68]}$	$0.002^{+0.000+0.005+0.011+0.000}_{-0.000-0.009-0.012-0.000}$	$-0.018^{+0.000+0.001+0.013+0.000}_{-0.000-0.000-0.014-0.001}$
$\langle S_3 \rangle_{[1,6]}$	$0.001^{+0.000+0.001+0.004+0.001}_{-0.000-0.001-0.005-0.001}$	$-0.004^{+0.000+0.000+0.005+0.001}_{-0.000-0.000-0.006-0.001}$
$\langle S_3 \rangle_{[1,2]}$	$0.000^{+0.000+0.005+0.003+0.005}_{-0.000-0.002-0.004-0.007}$	$0.004^{+0.000+0.000+0.002+0.004}_{-0.000-0.000-0.002-0.005}$
$\langle S_3 \rangle_{[4.3,6]}$	$0.002^{+0.000+0.004+0.009+0.000}_{-0.000-0.006-0.009-0.000}$	$-0.011^{+0.000+0.000+0.010+0.000}_{-0.000-0.000-0.011-0.000}$
$\langle S_3 \rangle_{[6,8]}$	$0.002^{+0.000+0.005+0.012+0.000}_{-0.000-0.009-0.012-0.000}$	$-0.020^{+0.000+0.001+0.014+0.000}_{-0.000-0.001-0.015-0.001}$
$\langle S_4 \rangle_{[0.1,2]}$	$-0.072^{+0.003+0.028+0.006+0.001}_{-0.003-0.007-0.006-0.001}$	$-0.067^{+0.004+0.000+0.008+0.002}_{-0.003-0.000-0.006-0.002}$
$\langle S_4 \rangle_{[2,4.3]}$	$0.098^{+0.007+0.040+0.025+0.001}_{-0.006-0.050-0.024-0.001}$	$0.123^{+0.007+0.004+0.022+0.001}_{-0.006-0.005-0.024-0.001}$
$\langle S_4 \rangle_{[4.3,8.68]}$	$0.212^{+0.003+0.022+0.014+0.001}_{-0.002-0.086-0.015-0.001}$	$0.236^{+0.002+0.003+0.012+0.001}_{-0.002-0.004-0.014-0.001}$
$\langle S_4 \rangle_{[1,6]}$	$0.102^{+0.007+0.036+0.024+0.001}_{-0.006-0.049-0.023-0.001}$	$0.125^{+0.006+0.003+0.021+0.001}_{-0.006-0.004-0.023-0.001}$
$\langle S_4 \rangle_{[1,2]}$	$-0.042^{+0.008+0.013+0.021+0.002}_{-0.006-0.007-0.016-0.002}$	$-0.023^{+0.009+0.000+0.020+0.002}_{-0.006-0.000-0.019-0.002}$
$\langle S_4 \rangle_{[4.3,6]}$	$0.186^{+0.004+0.034+0.017+0.001}_{-0.003-0.083-0.018-0.001}$	$0.212^{+0.003+0.004+0.015+0.000}_{-0.003-0.005-0.017-0.001}$
$\langle S_4 \rangle_{[6,8]}$	$0.221^{+0.002+0.018+0.012+0.001}_{-0.002-0.088-0.013-0.001}$	$0.245^{+0.001+0.002+0.011+0.001}_{-0.002-0.003-0.012-0.001}$
$\langle S_5 \rangle_{[0.1,2]}$	$0.207^{+0.004+0.008+0.012+0.004}_{-0.007-0.061-0.016-0.005}$	$0.211^{+0.006+0.000+0.013+0.005}_{-0.009-0.001-0.018-0.005}$
$\langle S_5 \rangle_{[2,4.3]}$	$-0.167^{+0.018+0.068+0.040+0.006}_{-0.025-0.038-0.035-0.007}$	$-0.172^{+0.016+0.006+0.034+0.005}_{-0.023-0.004-0.032-0.006}$
$\langle S_5 \rangle_{[4.3,8.68]}$	$-0.424^{+0.011+0.157+0.018+0.002}_{-0.019-0.021-0.015-0.002}$	$-0.406^{+0.010+0.007+0.019+0.002}_{-0.016-0.005-0.018-0.002}$
$\langle S_5 \rangle_{[1,6]}$	$-0.178^{+0.016+0.069+0.038+0.005}_{-0.027-0.040-0.033-0.006}$	$-0.177^{+0.015+0.005+0.032+0.005}_{-0.024-0.004-0.031-0.006}$
$\langle S_5 \rangle_{[1,2]}$	$0.149^{+0.016+0.011+0.039+0.007}_{-0.023-0.045-0.041-0.008}$	$0.135^{+0.018+0.003+0.038+0.007}_{-0.024-0.004-0.041-0.008}$
$\langle S_5 \rangle_{[4.3,6]}$	$-0.369^{+0.011+0.148+0.023+0.002}_{-0.024-0.038-0.020-0.002}$	$-0.359^{+0.010+0.009+0.022+0.002}_{-0.020-0.007-0.021-0.002}$
$\langle S_5 \rangle_{[6,8]}$	$-0.445^{+0.011+0.161+0.016+0.002}_{-0.021-0.019-0.015-0.001}$	$-0.424^{+0.010+0.006+0.019+0.002}_{-0.018-0.004-0.018-0.001}$
$\langle S_{6s} \rangle_{[0.1,2]}$	$0.174^{+0.002+0.078+0.006+0.000}_{-0.003-0.09\ -0.007-0.000}$	$0.163^{+0.003+0.008+0.007+0.001}_{-0.005-0.009-0.009-0.001}$
$\langle S_{6s} \rangle_{[2,4.3]}$	$0.105^{+0.018+0.113+0.044+0.005}_{-0.026-0.069-0.043-0.007}$	$0.062^{+0.017+0.005+0.044+0.005}_{-0.023-0.005-0.039-0.006}$
$\langle S_{6s} \rangle_{[4.3,8.68]}$	$-0.235^{+0.018+0.173+0.034+0.003}_{-0.032-0.231-0.030-0.003}$	$-0.273^{+0.016+0.018+0.033+0.003}_{-0.027-0.016-0.025-0.003}$
$\langle S_{6s} \rangle_{[1,6]}$	$0.055^{+0.016+0.036+0.042+0.004}_{-0.029-0.033-0.041-0.006}$	$0.017^{+0.013+0.001+0.042+0.004}_{-0.025-0.001-0.037-0.005}$
$\langle S_{6s} \rangle_{[1,2]}$	$0.265^{+0.008+0.28\ +0.025+0.003}_{-0.014-0.171-0.028-0.005}$	$0.231^{+0.013+0.018+0.024+0.004}_{-0.017-0.020-0.027-0.005}$
$\langle S_{6s} \rangle_{[4.3,6]}$	$-0.116^{+0.015+0.089+0.042+0.003}_{-0.033-0.161-0.038-0.003}$	$-0.159^{+0.013+0.012+0.041+0.002}_{-0.026-0.011-0.033-0.003}$
$\langle S_{6s} \rangle_{[6,8]}$	$-0.270^{+0.017+0.198+0.031+0.003}_{-0.037-0.246-0.028-0.003}$	$-0.309^{+0.015+0.020+0.030+0.003}_{-0.030-0.017-0.022-0.004}$

Table 6. SM predictions for F_L, S_3, S_4, S_5, S_{6s} in various bins. Same notation as table 3.

References

[1] LHCb collaboration, *Differential branching fraction and angular analysis of the decay $B^0 \to K^{*0}\mu^+\mu^-$*, *JHEP* **08** (2013) 131 [arXiv:1304.6325] [INSPIRE].

[2] LHCb collaboration, *Measurement of Form-Factor-Independent Observables in the Decay $B^0 \to K^{*0}\mu^+\mu^-$*, *Phys. Rev. Lett.* **111** (2013) 191801 [arXiv:1308.1707] [INSPIRE].

[3] S. Descotes-Genon, J. Matias, M. Ramon and J. Virto, *Implications from clean observables for the binned analysis of $B \to K^*\mu^+\mu^-$ at large recoil*, *JHEP* **01** (2013) 048 [arXiv:1207.2753] [INSPIRE].

[4] D. Becirevic and E. Schneider, *On transverse asymmetries in $B \to K^*\ell^+\ell^-$*, *Nucl. Phys.* **B 854** (2012) 321 [arXiv:1106.3283] [INSPIRE].

[5] J. Matias, F. Mescia, M. Ramon and J. Virto, *Complete Anatomy of $\bar{B}_d \to \bar{K}^{*0}(\to K\pi)l^+l^-$ and its angular distribution*, *JHEP* **04** (2012) 104 [arXiv:1202.4266] [INSPIRE].

[6] W. Altmannshofer, P. Ball, A. Bharucha, A.J. Buras, D.M. Straub et al., *Symmetries and Asymmetries of $B \to K^*\mu^+\mu^-$ Decays in the Standard Model and Beyond*, *JHEP* **01** (2009) 019 [arXiv:0811.1214] [INSPIRE].

[7] S. Descotes-Genon, J. Matias and J. Virto, *Understanding the $B \to K^*\mu^+\mu^-$ Anomaly*, *Phys. Rev.* **D 88** (2013) 074002 [arXiv:1307.5683] [INSPIRE].

[8] W. Altmannshofer and D.M. Straub, *New physics in $B \to K^*\mu\mu$?*, *Eur. Phys. J.* **C 73** (2013) 2646 [arXiv:1308.1501] [INSPIRE].

[9] F. Beaujean, C. Bobeth and D. van Dyk, *Comprehensive Bayesian analysis of rare (semi)leptonic and radiative B decays*, *Eur. Phys. J.* **C 74** (2014) 2897 [arXiv:1310.2478] [INSPIRE].

[10] L. Hofer, D. Scherer and L. Vernazza, *$B_s \to \phi\rho^0$ and $B_s \to \phi\pi^0$ as a handle on isospin-violating New Physics*, *JHEP* **02** (2011) 080 [arXiv:1011.6319] [INSPIRE].

[11] L. Hofer and L. Vernazza, *Status of the $B \to \pi K$ puzzle and its relation to $B_s \to \phi\pi$ and $B_s \to \phi\rho$ decays*, arXiv:1212.4785 [INSPIRE].

[12] W. Altmannshofer, S. Gori, M. Pospelov and I. Yavin, *Quark flavor transitions in $L_\mu - L_\tau$ models*, *Phys. Rev.* **D 89** (2014) 095033 [arXiv:1403.1269] [INSPIRE].

[13] F. Mahmoudi, S. Neshatpour and J. Virto, *$B \to K^*\mu^+\mu^-$ optimised observables in the MSSM*, *Eur. Phys. J.* **C 74** (2014) 2927 [arXiv:1401.2145] [INSPIRE].

[14] P. Biancofiore, P. Colangelo and F. De Fazio, *Rare semileptonic $B \to K^*\ell^+\ell^-$ decays in RS_c model*, *Phys. Rev.* **D 89** (2014) 095018 [arXiv:1403.2944] [INSPIRE].

[15] A.J. Buras, F. De Fazio and J. Girrbach-Noe, *Z-Z' mixing and Z-mediated FCNCs in $SU(3)_C \times SU(3)_L \times U(1)_X$ models*, *JHEP* **08** (2014) 039 [arXiv:1405.3850] [INSPIRE].

[16] A. Datta, M. Duraisamy and D. Ghosh, *Explaining the $B \to K^*\mu^+\mu^-$ data with scalar interactions*, *Phys. Rev.* **D 89** (2014) 071501 [arXiv:1310.1937] [INSPIRE].

[17] T. Hurth and F. Mahmoudi, *On the LHCb anomaly in $B \to K^* \ell^+ \ell^-$*, *JHEP* **04** (2014) 097 [arXiv:1312.5267] [InSPIRE].

[18] R. Gauld, F. Goertz and U. Haisch, *On minimal Z' explanations of the $B \to K*\mu^+\mu^-$ anomaly*, *Phys. Rev.* **D 89** (2014) 015005 [arXiv:1308.1959] [InSPIRE].

[19] R. Gauld, F. Goertz and U. Haisch, *An explicit Z'-boson explanation of the $B \to K^*\mu^+\mu^-$ anomaly*, *JHEP* **01** (2014) 069 [arXiv:1310.1082] [InSPIRE].

[20] A.J. Buras, F. De Fazio and J. Girrbach, *331 models facing new $b \to s\mu^+\mu^-$ data*, *JHEP* **02** (2014) 112 [arXiv:1311.6729] [InSPIRE].

[21] A.J. Buras and J. Girrbach, *Left-handed Z' and Z FCNC quark couplings facing new $b \to s\mu^+\mu^-$ data*, *JHEP* **12** (2013) 009 [arXiv:1309.2466] [InSPIRE].

[22] R.R. Horgan, Z. Liu, S. Meinel and M. Wingate, *Lattice QCD calculation of form factors describing the rare decays $B \to K^*\ell^+\ell^-$ and $B_s \to \phi\ell^+\ell^-$*, *Phys. Rev.* **D 89** (2014) 094501 [arXiv:1310.3722] [InSPIRE].

[23] R.R. Horgan, Z. Liu, S. Meinel and M. Wingate, *Calculation of $B^0 \to K^{*0}\mu^+\mu^-$ and $B_s^0 \to \phi\mu^+\mu^-$ observables using form factors from lattice QCD*, *Phys. Rev. Lett.* **112** (2014) 212003 [arXiv:1310.3887] [InSPIRE].

[24] S. Descotes-Genon, J. Matias and J. Virto, *Optimizing the basis of $B \to K^* l^+ l^-$ observables and understanding its tensions*, PoS(EPS-HEP 2013)361 [arXiv:1311.3876] [InSPIRE].

[25] A. Khodjamirian, T. Mannel, A.A. Pivovarov and Y.-M. Wang, *Charm-loop effect in $B \to K^{(*)}\ell^+\ell^-$ and $B \to K^*\gamma$*, *JHEP* **09** (2010) 089 [arXiv:1006.4945] [InSPIRE].

[26] BES collaboration, J.Z. Bai et al., *Measurements of the cross-section for $e^+e \to hadrons$ at center-of-mass energies from 2-GeV to 5-GeV*, *Phys. Rev. Lett.* **88** (2002) 101802 [hep-ex/0102003] [InSPIRE].

[27] LHCb collaboration, *Angular analysis of charged and neutral $B \to K\mu^+\mu^-$ decays*, *JHEP* **05** (2014) 082 [arXiv:1403.8045] [InSPIRE].

[28] J. Lyon and R. Zwicky, *Resonances gone topsy turvy - the charm of QCD or new physics in $b \to s\ell^+\ell^-$?*, arXiv:1406.0566 [InSPIRE].

[29] M. Beneke and T. Feldmann, *Symmetry breaking corrections to heavy to light B meson form-factors at large recoil*, *Nucl. Phys.* **B 592** (2001) 3 [hep-ph/0008255] [InSPIRE].

[30] M. Beneke, T. Feldmann and D. Seidel, *Systematic approach to exclusive $B \to V\ell^+\ell^-$, V gamma decays*, *Nucl. Phys.* **B 612** (2001) 25 [hep-ph/0106067] [InSPIRE].

[31] B. Grinstein and D. Pirjol, *Exclusive rare $B \to K^*\ell^+\ell^-$ decays at low recoil: Controlling the long-distance effects*, *Phys. Rev.* **D 70** (2004) 114005 [hep-ph/0404250] [InSPIRE].

[32] J. Charles, A. Le Yaouanc, L. Oliver, O. Pene and J.C. Raynal, *Heavy to light form-factors in the heavy mass to large energy limit of QCD*, *Phys. Rev.* **D 60** (1999) 014001 [hep-ph/9812358] [InSPIRE].

[33] C.W. Bauer, S. Fleming, D. Pirjol and I.W. Stewart, *An Effective field theory for collinear and soft gluons: Heavy to light decays*, *Phys. Rev.* **D 63** (2001) 114020 [hep-ph/0011336] [InSPIRE].

[34] F. Krüger and J. Matias, *Probing new physics via the transverse amplitudes of $B^0 \to K^0(\to K^-\pi^+)\ell^+\ell^-$ at large recoil*, *Phys. Rev.* **D 71** (2005) 094009 [hep-ph/0502060] [InSPIRE].

[35] U. Egede, T. Hurth, J. Matias, M. Ramon and W. Reece, *New observables in the decay mode* $\bar{B}_d \to \bar{K}^0 \ell^+ \ell^-$, *JHEP* **11** (2008) 032 [arXiv:0807.2589] [INSPIRE].

[36] U. Egede, T. Hurth, J. Matias, M. Ramon and W. Reece, *New physics reach of the decay mode* $\bar{B} \to \bar{K}^{*0} \ell^+ \ell^-$, *JHEP* **10** (2010) 056 [arXiv:1005.0571] [INSPIRE].

[37] C. Bobeth, G. Hiller and D. van Dyk, *The Benefits of* $\bar{B} \to \bar{K}^* l^+ l^-$ *Decays at Low Recoil*, *JHEP* **07** (2010) 098 [arXiv:1006.5013] [INSPIRE].

[38] C. Bobeth, G. Hiller and D. van Dyk, *More Benefits of Semileptonic Rare B Decays at Low Recoil: CP-violation*, *JHEP* **07** (2011) 067 [arXiv:1105.0376] [INSPIRE].

[39] S. Descotes-Genon, T. Hurth, J. Matias and J. Virto, *Optimizing the basis of* $B \to K^* \ell^+ \ell^-$ *observables in the full kinematic range*, *JHEP* **05** (2013) 137 [arXiv:1303.5794] [INSPIRE].

[40] S. Descotes-Genon, D. Ghosh, J. Matias and M. Ramon, *Exploring New Physics in the C7-C7' plane*, *JHEP* **06** (2011) 099 [arXiv:1104.3342] [INSPIRE].

[41] S. Jäger and J. Martin Camalich, *On* $B \to V ll$ *at small dilepton invariant mass, power corrections and new physics*, *JHEP* **05** (2013) 043 [arXiv:1212.2263] [INSPIRE].

[42] PARTICLE DATA GROUP collaboration, J. Beringer et al., *Review of Particle Physics (RPP)*, *Phys. Rev.* **D 86** (2012) 010001 [INSPIRE].

[43] M. Beneke, T. Feldmann and D. Seidel, *Exclusive radiative and electroweak* $b \to d$ *and* $b \to s$ *penguin decays at NLO*, *Eur. Phys. J.* **C 41** (2005) 173 [hep-ph/0412400] [INSPIRE].

[44] P. Ball and R. Zwicky, *New results on* $B \to pi, K, \eta$ *decay formfactors from light-cone sum rules*, *Phys. Rev.* **D 71** (2005) 014015 [hep-ph/0406232] [INSPIRE].

[45] E. Lunghi and J. Matias, *Huge right-handed current effects in* $B \to K*(K\pi)\ell^+\ell^-$ *in supersymmetry*, *JHEP* **04** (2007) 058 [hep-ph/0612166] [INSPIRE].

[46] CDF collaboration, T. Aaltonen et al., *Measurements of the Angular Distributions in the Decays* $B \to K^{(*)}\mu^+\mu^-$ *at CDF*, *Phys. Rev. Lett.* **108** (2012) 081807 [arXiv:1108.0695] [INSPIRE].

[47] CDF collaboration, S. Behari, *CDF results on* $b \to s\mu\mu$ *decays*, arXiv:1301.2244 [INSPIRE].

[48] J. Matias and N. Serra, *A new relation between the zero of* A_{FB} *in* $B^0 \to K^*\mu^+\mu^-$ *and the anomaly in* P_5', *Phys. Rev.* **D 90** (2014) 034002 [arXiv:1402.6855] [INSPIRE].

[49] A. Ali, A.Y. Parkhomenko and A.V. Rusov, *Precise Calculation of the Dilepton Invariant-Mass Spectrum and the Decay Rate in* $B^{\pm} \to \pi^{\pm}\mu^+\mu^-$ *in the SM*, *Phys. Rev.* **D 89** (2014) 094021 [arXiv:1312.2523] [INSPIRE].

[50] J. Lyon and R. Zwicky, *Isospin asymmetries in* $B \to (K^*, \rho)\gamma/l^+l^-$ *and* $B \to Kl^+l^-$ *in and beyond the standard model*, *Phys. Rev.* **D 88** (2013) 094004 [arXiv:1305.4797] [INSPIRE].

[51] LHCb collaboration, *First observation of the decay* $B^+ \to \pi^+\mu^+\mu^-$, *JHEP* **12** (2012) 125 [arXiv:1210.2645] [INSPIRE].

[52] R.N. Faustov and V.O. Galkin, *Rare* $B \to \pi l\bar{l}$ *and* $B \to \rho l\bar{l}$ *decays in the relativistic quark model*, *Eur. Phys. J.* **C 74** (2014) 2911 [arXiv:1403.4466] [INSPIRE].

[53] A. Khodjamirian, T. Mannel and Y.M. Wang, $B \to K\ell^+\ell^-$ *decay at large hadronic recoil*, *JHEP* **02** (2013) 010 [arXiv:1211.0234] [INSPIRE].